NUMERICAL ANALYSIS AND DIMENSION SPLITTING FOR A SEMI-LAGRANGIAN DISCONTINUOUS FINITE ELEMENT SCHEME BASED ON THE CHARACTERISTIC GALERKIN METHOD

ZHENGRONG XIE

Abstract. A semi-Lagrangian discontinuous finite element scheme based on the characteristic Galerkin method (CSLDG) is investigated, which directly discretizes an integral invariant model derived from the coupling of the transport equation and its adjoint equation. First, the existence and stability of CSLDG are proven, along with the uniqueness of the numerical solution. Subsequently, in contrast to the commonly used interpolation-based dimensional splitting schemes (IBS) within the CSLDG framework, a separated-variable dimensional splitting approach based on the tensor product (SVS) is proposed and applied to the two-dimensional case. Numerical experiments show comparable accuracy between methods, but SVS demonstrates superior computational efficiency to IBS, especially on large-scale meshes.

Contents

Date: March 3, 2026.

2020 *Mathematics Subject Classification.* 35L04, 65M12, 65M25, 65M60.

Key words and phrases. SLDG; Numerical Existence; Numerical Stability; Numerical Uniqueness; Separated Variable's Splitting.

1. Introduction

Consider the following linear scalar transport equation:

$$\begin{cases} U_t + \nabla \cdot (\mathbf{A}(\mathbf{x},t)U) = 0 \quad \text{in} \quad \Omega \times [0,T], \\ \text{I.C.} \quad U(\mathbf{x},0) = U_0(\mathbf{x}), \quad \mathbf{x} \in \Omega. \end{cases} \tag{1.1}$$

Here, T is an arbitrary positive constant, and $\Omega \subset \mathbb{R}^d$ is a bounded domain. The vector function $\mathbf{A}(\mathbf{x},t) = (a_1(\mathbf{x},t), a_2(\mathbf{x},t), \ldots, a_d(\mathbf{x},t))^{\mathrm{T}}$ is assumed to be continuous with respect to both $\mathbf{x}$ and t, and its first-order partial derivatives are also continuous. The field function $U : \mathbb{R}^d \times [0,+\infty) \to \mathbb{R}$ is defined such that the initial field distribution U_0 belongs to the $L^2(\Omega)$ space.

The adjoint problem (adjoint equation) for the problem (1.1) is given by [1, 2]:

$$\begin{cases} \psi_t + \mathbf{A}(\mathbf{x},t) \cdot \nabla \psi = 0 \quad \text{in} \quad \Omega \times [0,T], \\ \text{F.C.} \quad \psi(\mathbf{x},T) = \Psi(\mathbf{x}), \quad \mathbf{x} \in \Omega. \end{cases} \tag{1.2}$$

The characteristic equation associated with Equation (1.2) is given by:

$$\frac{\mathrm{d}\mathbf{x}}{\mathrm{d}t} = \mathbf{A}(\mathbf{x},t), \tag{1.3}$$

which, in its expanded (component-wise) form, can be written as:

$$\frac{\mathrm{d}x_i}{\mathrm{d}t} = a_i(x_1, x_2, \ldots, x_i, \ldots, x_d, t), \quad i = 1, 2, \ldots, d. \tag{1.4}$$

Along the characteristic lines, ψ is preserved such that $\forall t_1, t_2 \in [0,T]$,

$$\psi(x_1^2, x_2^2, \ldots, x_i^2, \ldots, x_d^2, t_2) = \psi(x_1^1, x_2^1, \ldots, x_i^1, \ldots, x_d^1, t_1), \tag{1.5}$$

where $(x_1^2, x_2^2, \ldots, x_i^2, \ldots, x_d^2, t_2)$ and $(x_1^1, x_2^1, \ldots, x_i^1, \ldots, x_d^1, t_1)$ satisfy the following system:

$$\begin{cases} \dfrac{\mathrm{d}x_i}{\mathrm{d}t} = a_i(x_1, x_2, \ldots, x_i, \ldots, x_d, t), \\ x_i(t_2) = x_i^2, \\ x_i(t_1) = x_i^1, \\ i = 1, 2, \ldots, d. \end{cases} \tag{1.6}$$

To achieve long-time, large-time-step, and unconditionally stable solutions for Problem (1.1), a widely adopted approach is the semi-Lagrangian discontinuous finite element scheme based on the characteristic Galerkin framework (CSLDG) [1, 3, 4]. The core idea of this method lies in the numerical solution of the following integral invariant:

$$\frac{\mathrm{d}}{\mathrm{d}t} \int_{\widetilde{\Omega}(t)} U(\mathbf{x},t)\psi(\mathbf{x},t)\,\mathrm{d}\mathbf{x} = 0, \tag{1.7}$$

where $\widetilde{\Omega}(t)$ represents the characteristic space-time region emanating from the characteristic lines, as illustrated in Figure 1. By combining Eq. (1.1) and Eq. (1.2) and applying the

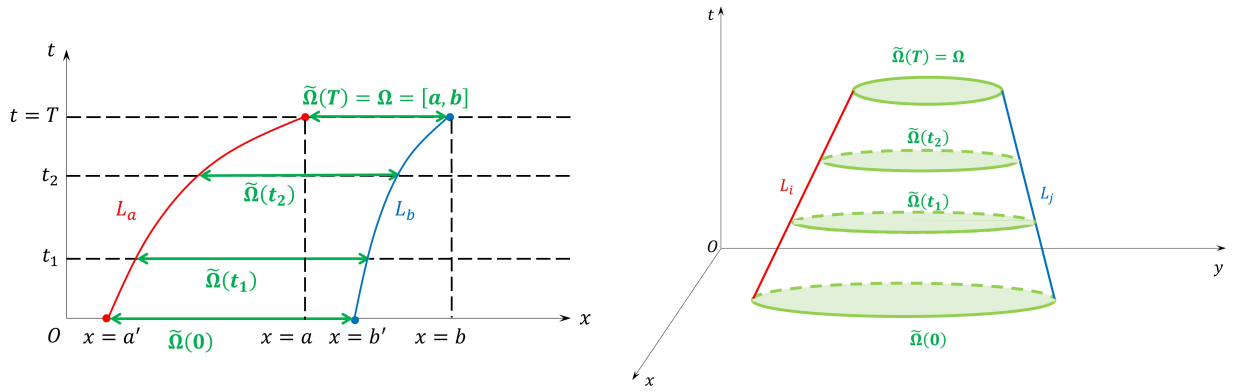

(a) $\Omega \subset \mathbb{R}$ (b) $\Omega \subset \mathbb{R}^2$

FIGURE 1. Characteristic Dynamic Domain.

differentiation formula for integrals with variable limits, also known as the Leibniz rule (see Appendix A), the integral invariant in Eq. (1.7) can be readily established [1]. From a computational standpoint, it is observed that the domain $\widetilde{\Omega}(0)$ may be partially or completely deformed outside Ω through the motion. Since the initial field distribution defined on $\widetilde{\Omega}(0)$ is required for initiating the time-stepping recursive computation, the initial condition $\widetilde{U}^0$ must be properly extended to the entire $\widetilde{\Omega}(0)$. To achieve this extension, periodic boundary conditions are typically implemented together with virtual grid techniques in the discrete computational framework. The initial values are thus supplemented in a numerically consistent manner. From a strictly computational perspective, it should be noted that the subsequent simulation can be successfully advanced as long as appropriate sampled values are provided on $\widetilde{\Omega}(0) \setminus \Omega$. Therefore, inflow boundary conditions may be imposed, or alternatively, simpler compact-support constraints can be adopted for numerical convenience. It is worth noting, however, that virtually all existing CSLDG and even FSLDG papers adopt either periodic boundary conditions or a compact-support assumption; inflow boundary conditions have been addressed only in Ref[5]. Consequently, the theoretical analysis in this work focuses on periodic or compactly supported settings.

An essential condition for the validity of this method is evidently the non-intersection of characteristic lines, meaning that without special treatment, the method is not applicable to problems with discontinuities. Therefore, if we denote the time at which discontinuities appear in the adjoint equation (1.2) (i.e., the intersection of characteristic lines) as T^*, we require

$$T < T^* \ (T^* \leq \infty), \tag{1.8}$$

where $T^* = \infty$ implies that the characteristic lines never intersect, and the entire flow field remains smooth without discontinuities, e.g., incompressible flow with $\nabla \cdot \mathbf{A} = 0$. In this case, no upper limit is imposed on T.

The CSLDG method examined in this paper has seen significant development and application. References [1] extended this CSLDG from one dimension to two dimensions via dimensional splitting and applied it to solve the Vlasov system [6, 7] and the incompressible Euler equations [4]. Reference [8] combined the aforementioned CSLDG with the local discontinuous Galerkin method (LDG) and directly approximated the upstream elements using two-dimensional straight-edged meshes. This approach avoided splitting errors associated with dimensional splitting and the "convection-diffusion operator splitting," successfully solving the scalar convection-diffusion equation. Cai et al. further enhanced the accuracy of this CSLDG by implementing it on curved meshes using a parametric mapping technique [9, 10].

The research on this CSLDG method with the integral invariant formulation in Eq.(1.7), is currently mainly focused on algorithm construction and numerical simulation. However, the existence and uniqueness of the numerical solutions, the stability of the numerical scheme, and the priori estimates of the convergence order have not yet been established. Although the method is inspired by the Eulerian-Lagrangian localized adjoint method (ELLAM), which has a longer history and more theoretical analysis [2, 11, 12], the proof methods and results in the ELLAM framework are not directly applicable to this CSLDG method.

It is essential to emphasize that, in addition to the CSLDG algorithm, there exists another category of semi-Lagrangian discontinuous Galerkin algorithm in the flux difference form [13, 14] (hereinafter referred to as the FSLDG). The numerical stability, optimal convergence rates, and superconvergence properties of the FSLDG have all been demonstrated [13, 15, 16]. It should be noted that the analysis of the FSLDG does not cover the theoretical issues related to the weak solutions and numerical solutions of the CSLDG.

In this paper, the existence and uniqueness of the numerical solution for CSLDG, as well as the numerical stability of this scheme, are established for the first time within the framework of mathematical induction. The proof relies on the Riesz Representation Theorem and skillfully utilizes the compact-support of the time-dependent test functions. Additionally, inspired by [17], we construct a two-dimensional orthogonal basis on rectangular grids using the tensor product of one-dimensional orthogonal polynomials. This allows us to express the DG approximate solution in a separated form with respect to the x and y variables. Based on this foundation, we propose a new implementation scheme for the two dimensional CSLDG framework, which is applicable to arbitrary-order dimensional splitting schemes.

The paper is organized as follows: Section 2 reviews the implementation of the CSLDG method using the one-dimensional scalar transport equation as an example. Section 3 discusses the existence, stability, and uniqueness of the numerical solution of the CSLDG. Section 4 introduces a new method for implementing dimensional splitting in the CSLDG

framework based on the tensor product of two-dimensional orthogonal bases. The effectiveness of the work in Section 4 is verified by numerical experiments in Section 5. Section 6 summarizes and concludes the paper.

2. Overview of CSLDG

2.1. **Basic Assumptions.**

To accurately define and describe the CSLDG algorithm and facilitate subsequent numerical analysis, we need to make certain a priori assumptions. These assumptions will be used directly in defining the numerical solution of the CSLDG scheme and in proving the key lemmas presented in the following subsection **??**.

First, assume that the velocity field $\mathbf{A}(\mathbf{x}, t)$ in the linear scalar transport equation(1.1) satisfies a uniformly bounded gradient condition, i.e., there exists a constant $L_A > 0$ such that for all $\mathbf{x} \in \mathbb{R}^d$ and $\tau \in [0, T]$, the following holds:

$$\sup_{\mathbf{x}\in\mathbb{R}^d, t\in[0,T]} \|\nabla_{\mathbf{x}}\mathbf{A}(\mathbf{x}, t)\|_{\text{op}} \leq L_A, \tag{2.1}$$

where $\nabla_{\mathbf{x}}\mathbf{A}(\mathbf{x}, t)$ is the Jacobian matrix of $\mathbf{A}$ with respect to the spatial variables $\mathbf{x}$. $\|\cdot\|_{\text{op}}$ denotes the operator norm of a matrix, defined as:

$$\|\nabla_{\mathbf{x}}\mathbf{A}\|_{\text{op}} = \sup_{\|\mathbf{v}\|=1} \|(\nabla_{\mathbf{x}}\mathbf{A})\,\mathbf{v}\|\,.$$

This norm is equivalent to the largest singular value (spectral norm) of the Jacobian matrix. It is important to note that the **uniformly bounded gradient** condition implies that $\mathbf{A}$ satisfies the **linear growth condition**. Specifically, there exist continuous functions $\alpha(t)$ and $\beta(t)$ such that:

$$\|\mathbf{A}(\mathbf{x}, t)\| \leq \alpha(t) \cdot \|\mathbf{x}\| + \beta(t), \quad \forall (\mathbf{x}, t) \in \mathbb{R}^d \times [0, T]. \tag{2.2}$$

Furthermore, if the gradient of $\mathbf{A}$ is uniformly bounded, then **the divergence of A is necessarily uniformly bounded,** i.e., there exists $M_A > 0$ such that

$$\|\nabla_{\mathbf{x}} \cdot \mathbf{A}(\mathbf{x}, t)\|_{L^\infty(\mathbb{R}^d)} \leq M_A, \ \forall t \in [0, T]. \tag{2.3}$$

Here, a feasible choice for the upper bound M_A is $M_A = dL_A$. (Inspired by the relationship between the trace of a matrix and its row norm and operator norm)

As noted in Section 1, $\mathbf{A}(\mathbf{x}, t)$ has **continuous first-order partial derivatives**, ensuring that both the Cauchy initial value problem and the terminal value problem for $\frac{\mathrm{d}\mathbf{s}}{\mathrm{d}\tau} = \mathbf{A}(\mathbf{s}, \tau)$ are **locally well-posed** (on the intervals $[0, \delta]$ and $[T-\delta, T]$, respectively, with δ sufficiently small). Furthermore, when combined with the **linear growth constraint** (2.2) resulting from the **uniformly bounded gradient condition** (2.1), the solutions to the Cauchy initial/terminal value problems for $\frac{\mathrm{d}\mathbf{s}}{\mathrm{d}\tau} = \mathbf{A}(\mathbf{s}, \tau)$ can be extended to the entire interval $[0, T]$, i.e., they become **globally well-posed**. Therefore, for any fixed time $t \in [0, T]$ we can

define the flow mapping $\mathrm{D}^{\mathbf{A}}_{t\to T}$:

$$\begin{aligned}\mathrm{D}^{\mathbf{A}}_{T\to t}:\ &\Omega\to\widetilde{\Omega}(t)\\ &\mathbf{x}_T\mapsto\mathbf{x}_t=\mathbf{x}_T-\int_t^T\mathbf{A}(\mathbf{s}(\tau),\tau)\mathrm{d}\tau,\end{aligned}\tag{2.4}$$

where Ω is a bounded open domain in $\mathbb{R}^d$, and $\mathbf{s}(\tau)$ satisfies $\frac{\mathrm{d}\mathbf{s}}{\mathrm{d}\tau}=\mathbf{A}(\mathbf{s},\tau)$ with $\mathbf{s}(T)=\mathbf{x}_T$. Given that $\mathbf{A}$ is **continuously differentiable** ($\mathbf{A}\in C^1$) and **its gradient is uniformly bounded**, it further follows that **the flow map** $\mathrm{D}^{\mathbf{A}}_{T\to t}$ **is invertible** and its inverse operator is given by

$$\begin{aligned}\mathrm{D}^{\mathbf{A}}_{t\to T}:\ &\widetilde{\Omega}(t)\to\Omega\\ &\mathbf{x}_t\mapsto\mathbf{x}_T=\mathbf{x}_t+\int_t^T\mathbf{A}(\mathbf{s}(\tau),\tau)\mathrm{d}\tau,\end{aligned}\tag{2.5}$$

where $\mathbf{s}(\tau)$ satisfies $\frac{\mathrm{d}\mathbf{s}}{\mathrm{d}\tau}=\mathbf{A}(\mathbf{s},\tau)$ with $\mathbf{s}(t)=\mathbf{x}_t$. Therefore, under the action of the reversible mapping $\mathrm{D}^{\mathbf{A}}_{T\rightleftarrows t}(\cdot)$, the regions Ω and $\widetilde{\Omega}(t)$ are **diffeomorphic** ($\Omega\cong\widetilde{\Omega}(t)$). By the composition property of the flow mapping $\mathrm{D}^{\mathbf{A}}_{T\to t}(\cdot)$ and the transitivity of diffeomorphisms, it follows that for any $t^\star,t^\dagger\in[0,T]$:

$$\widetilde{\Omega}(t^\star)=\mathrm{D}^{\mathbf{A}}_{t^\dagger\to t^\star}\left(\widetilde{\Omega}(t^\dagger)\right),\tag{2.6a}$$

$$\widetilde{\Omega}(t^\star)\cong\widetilde{\Omega}(t^\dagger).\tag{2.6b}$$

Remark 2.1. *The invertibility of the flow map* $\mathrm{D}^{\mathbf{A}}_{T\to t}$ *directly guarantees the validity of the change of variables in the proof of Lemma 3.2, i.e.,*

$$\left|\det J_{\mathrm{D}^{\mathbf{A}}_{T\to t}}(\mathbf{x}_T)\right|=\left|\det J_{\mathrm{D}^{\mathbf{A}}_{t\to T}}(\mathbf{x}_t)\right|^{-1}=\exp\left(\int_t^T\nabla\cdot\mathbf{A}(\mathbf{s}(\tau),\tau)d\tau\right)^{-1}=\exp\left(-\int_t^T\nabla\cdot\mathbf{A}(\mathbf{s}(\tau),\tau)d\tau\right)$$

is meaningful.

The symbols H, C^1, and L^2 are retained to represent their conventional mathematical meanings. For instance, H denotes the Hilbert space composed of L^2-functions and equipped with the L^2-inner product. Furthermore, H_0 denotes the Hilbert space under the L^2-inner product with compact-support on a bounded domain Ω, i.e.,

$$\begin{aligned}H_0(\Omega)&:=\left\{f\in L^2(\mathbb{R}^d):\mathrm{supp}\{f\}\subset\subset\Omega\right\},\\ \langle f,g\rangle&:=\int_{\mathbb{R}^d}fg\,\mathrm{d}x=\int_\Omega fg\,\mathrm{d}x,\quad f,g\in H_0(\Omega).\end{aligned}$$

Remark 2.2 ($H_0(\Omega)\subset H(\mathbb{R}^d)$)**.** *Let* $H(\mathbb{R}^d)$ *denote the Hilbert space formed by the* L^2*-space defined on the entire domain* $\mathbb{R}^d$ *equipped with the* L^2*-inner product. Let* $\mathcal{D}(\Omega)$ *denote the set of all functions with compact-support in* Ω*. Then,* $H_0(\Omega)=H(\mathbb{R}^d)\cap\mathcal{D}(\Omega)$.

Define the following **function evolution operator** (an explicit time-dependent transformation):

$$\Phi^{\mathbf{A}}_{T\to t}[f_T](\mathbf{x}_t) := f_T(\mathrm{D}^{\mathbf{A}}_{t\to T}(\mathbf{x}_t)) = f_T(\mathbf{x}_t + \int_t^T \mathbf{A}(\mathbf{s}(\tau),\tau)\ \mathrm{d}\tau),\ \ \mathbf{x}_t \in \widetilde{\Omega}(t),\ \ t\in[0,T],\ \ f_T \in L^2(\Omega). \tag{2.7}$$

where $\mathbf{s}(\tau)$ satisfies $\frac{\mathrm{d}\mathbf{s}}{\mathrm{d}\tau} = \mathbf{A}(\mathbf{s},\tau)$ with $\mathbf{s}(t) = \mathbf{x}_t$. It is straightforward to verify the composition property of this operator: for any $t^\star, t^\dagger \in [0,T]$ it holds that

$$\Phi^{\mathbf{A}}_{T\to t^\star}[f_T](\mathbf{x}) = \Phi^{\mathbf{A}}_{t^\dagger\to t^\star} \circ \Phi^{\mathbf{A}}_{T\to t^\dagger}[f_T](\mathbf{x}),\ \ \mathbf{x}\in\widetilde{\Omega}(t^\star). \tag{2.8}$$

Analogous to $\mathrm{D}^{\mathbf{A}}_{T\to t}(\cdot)$, since both the Cauchy initial value problem and Cauchy terminal value problem for $\frac{\mathrm{d}\mathbf{s}}{\mathrm{d}\tau} = \mathbf{A}(\mathbf{s},\tau)$ are well-posed, as well as the gradient of $\mathbf{A}(\mathbf{x},t)$ is uniformly bounded, the operator $\Phi^{\mathbf{A}}_{T\to t}[\cdot]$ is **invertible**. Denoting $f_t = \Phi^{\mathbf{A}}_{T\to t}[f_T](\mathbf{x}_t)$, we have:

$$f_T = \Phi^{\mathbf{A}}_{t\to T}[f_t](\mathbf{x}_T) = f_t\left(\mathbf{x}_T - \int_t^T \mathbf{A}(\mathbf{s}(\tau),\tau)\mathrm{d}\tau\right),\ \ \mathbf{x}_T\in\Omega, \tag{2.9}$$

where $\mathbf{s}(\tau)$ satisfies $\frac{\mathrm{d}\mathbf{s}}{\mathrm{d}\tau} = \mathbf{A}(\mathbf{s},\tau)$ with $\mathbf{s}(T) = \mathbf{x}_T$.

2.2. **Notations and Definitions.**

This subsection introduces the notations used in the numerical discretization and provides the definition of the CSLDG numerical solution. These notations and definitions will recur throughout the subsequent analysis for proving the existence, uniqueness, and stability of the numerical solution.

Let $\mathcal{T}_h$ be a spatial partition of the computational domain Ω, such that $\mathcal{T}_h = \Omega_1 \cup \Omega_2 \cup \cdots \cup \Omega_{\mathcal{K}} \cup \cdots \cup \Omega_M$, where $\Omega_i \cap \Omega_j = \varnothing$ for all $i,j \in \{1,2,\ldots,M\}$. Additionally, a temporal partition is defined by $t_n = n\Delta t$ for $n = 0,1,2,\ldots,N$, where $\Delta t = T/N$.

Let $\widetilde{\Omega}^{n+1,n}_{\mathcal{K}}$ denote the bounded region obtained by mapping the element $\Omega_{\mathcal{K}}$ from time t_{n+1} to time t_n via the characteristic equation (1.3), i.e.,

$$\widetilde{\Omega}^{n+1,n}_{\mathcal{K}} = \mathrm{D}^{\mathbf{A}}_{t_{n+1}\to t_n}(\Omega_{\mathcal{K}}). \tag{2.10}$$

Let $\mathbb{D}\{\widetilde{\Omega}^{n+1,n}_{\mathcal{K}}\}$ represent the collection of all grid elements that intersect with $\widetilde{\Omega}^{n+1,n}_{\mathcal{K}}$, defined as

$$\mathbb{D}\{\widetilde{\Omega}^{n+1,n}_{\mathcal{K}}\} := \left\{\Omega_{\mathcal{K}_i} \in \mathcal{T}_h : \Omega_{\mathcal{K}_i} \cap \widetilde{\Omega}^{n+1,n}_{\mathcal{K}} \neq \varnothing\right\}. \tag{2.11}$$

Let

$$d_s := \left|\mathbb{D}\{\widetilde{\Omega}^{n+1,n}_{\mathcal{K}}\}\right| \tag{2.12}$$

denote the total number of grid elements intersecting with $\widetilde{\Omega}^{n+1,n}_{\mathcal{K}}$, where d_s depends on $(\Omega_{\mathcal{K}}, t_{n+1}, \Delta t, \mathbf{A}, \mathcal{T}_h)$. Note that

$$\left\{\Omega_{\mathcal{K}_i} \cap \widetilde{\Omega}^{n+1,n}_{\mathcal{K}}\right\} \cap \left\{\Omega_{\mathcal{K}_j} \cap \widetilde{\Omega}^{n+1,n}_{\mathcal{K}}\right\} = \varnothing, \quad \forall \Omega_{\mathcal{K}_i}, \Omega_{\mathcal{K}_j} \in \mathbb{D}\{\widetilde{\Omega}^{n+1,n}_{\mathcal{K}}\}. \tag{2.13}$$

Furthermore, let

$$\widetilde{\Omega}^{n+1,n} = \mathrm{D}^{\mathbf{A}}_{t_{n+1}\to t_n}(\Omega), \tag{2.14}$$

so that

$$\widetilde{\Omega}^{n+1,n} = \bigcup_{\Omega_{\mathcal{K}}\in\mathcal{T}_h} \widetilde{\Omega}^{n+1,n}_{\mathcal{K}}. \tag{2.15}$$

The discontinuous finite element solution U^n_h at time t_n is piecewise distributed discontinuously over the spatial partition $\mathcal{T}_h$. Let

$$U^n_i := U^n_h|_{\Omega_i}. \tag{2.16}$$

Hereafter, we always assume that U^n_i is defined over the entire space $\mathbb{R}^d$ but is extended by zero outside Ω_i, i.e., $\mathrm{supp}\{U^n_i\} \subset\subset \Omega_i$. This implies

$$U^n_i(\mathbf{x}) = U^n_h(\mathbf{x}) \cdot \chi_{\Omega_i}(\mathbf{x}), \tag{2.17}$$

where

$$\chi_{\Omega_i}(\mathbf{x}) = \begin{cases} 1, & \mathbf{x} \in \Omega_i, \\ 0, & \mathbf{x} \notin \Omega_i. \end{cases} \tag{2.18}$$

Consequently,

$$U^n_h = \sum_{\Omega_i\in\mathcal{T}_h} U^n_i, \tag{2.19}$$

and

$$\mathrm{supp}\{U^n_h\} \subset\subset \Omega. \tag{2.20}$$

The restriction of U^n_h over the collection $\mathbb{D}\{\widetilde{\Omega}^{n+1,n}_{\mathcal{K}}\}$ is denoted by $\mathbb{U}(\widetilde{\Omega}^{n+1,n}_{\mathcal{K}})$, i.e.,

$$\mathbb{U}(\widetilde{\Omega}^{n+1,n}_{\mathcal{K}}) = \{U^n_{\mathcal{K}_i} : \Omega_{\mathcal{K}_i} \cap \widetilde{\Omega}^{n+1,n}_{\mathcal{K}} \neq \varnothing\}. \tag{2.21}$$

The restriction of U^n_h on $\widetilde{\Omega}^{n+1,n}_{\mathcal{K}}$ is correspondingly denoted by $\widetilde{U}^n_{\mathcal{K}}$:

$$\widetilde{U}^n_{\mathcal{K}} := U^n_h|_{\widetilde{\Omega}^{n+1,n}_{\mathcal{K}}}. \tag{2.22}$$

Let

$$\widetilde{U}^n_{\mathcal{K},\mathcal{K}_i} := U^n_{\mathcal{K}_i} \cdot \chi_{\Omega_{\mathcal{K}_i}\cap\widetilde{\Omega}^{n+1,n}_{\mathcal{K}}}(\mathbf{x}), \quad \Omega_{\mathcal{K}_i} \in \mathbb{D}(\widetilde{\Omega}^{n+1,n}_{\mathcal{K}}), \tag{2.23}$$

where $\chi_{\Omega_{\mathcal{K}_i}\cap\widetilde{\Omega}^{n+1,n}_{\mathcal{K}}}$ is the characteristic function of the intersection region $\Omega_{\mathcal{K}_i} \cap \widetilde{\Omega}^{n+1,n}_{\mathcal{K}}$. Consequently,

$$\widetilde{U}^n_{\mathcal{K}} = \sum_{\Omega_{\mathcal{K}_i}\in\mathbb{D}\{\widetilde{\Omega}^{n+1,n}_{\mathcal{K}}\}} \widetilde{U}^n_{\mathcal{K},\mathcal{K}_i}, \tag{2.24}$$

which implies

$$\mathrm{supp}\{\widetilde{U}^n_{\mathcal{K}}\} \subset\subset \widetilde{\Omega}^{n+1,n}_{\mathcal{K}} \quad (\widetilde{U}^n_{\mathcal{K}} \text{ is extended by zero outside } \widetilde{\Omega}^{n+1,n}_{\mathcal{K}}). \tag{2.25}$$

Introduce the operator Π to represent the mapping from equations (2.16) to (2.24):

$$\widetilde{U}_{\mathcal{K}}^{n} = \Pi(U_h^n, \mathbb{D}\{\widetilde{\Omega}_{\mathcal{K}}^{n+1,n}\}). \tag{2.26}$$

Define

$$\widetilde{U}_h^n := \sum_{\Omega_{\mathcal{K}} \in \mathcal{T}_h} \widetilde{U}_{\mathcal{K}}^n, \tag{2.27}$$

which satisfies

$$\widetilde{U}_h^n|_{\widetilde{\Omega}_{\mathcal{K}}^{n+1,n}} = \widetilde{U}_{\mathcal{K}}^n \quad \text{i.e.,} \quad \widetilde{U}_h^n \cdot \chi_{\widetilde{\Omega}_{\mathcal{K}}^{n+1,n}} = \widetilde{U}_{\mathcal{K}}^n. \tag{2.28}$$

Remark 2.3. *The virtual grid technique is employed to extend the grid around the actual computational domain Ω, and the field function on the virtual grid is assigned according to periodic boundary conditions or compact-support constraints. This ensures the well-definedness of equations (2.11)-(2.28) on grid elements at the boundary $\partial\Omega$. This will not be explicitly mentioned hereafter.*

Now, the entire computational domain Ω is evolved according to the characteristic equation (1.3):

$$\widetilde{\Omega}(t) := \mathrm{D}_{T\to t}^{\mathbf{A}}(\Omega), \quad t \in [0, T], \tag{2.29}$$

noting that $\widetilde{\Omega}(T) = \Omega$. Let

$$\widehat{\Omega} = \bigcup_{t\in[0,T]} \widetilde{\Omega}(t), \tag{2.30}$$

where it is clear that $\widetilde{\Omega}(t) \subset \widehat{\Omega}$ for all $t \in [0, T]$. Additionally, let

$$\widetilde{Q}_T := \left\{\widetilde{\Omega}(t) : t \in [0, T]\right\}, \tag{2.31}$$

$$Q_T := \widehat{\Omega} \times [0, T], \tag{2.32}$$

then it follows that $\widetilde{Q}_T \subset Q_T$.

Definition 2.1 (CSLDG Numerical Solution Sequence)**.** *For a given initial value $U_0 \in L^2(\Omega)$, the sequence $\{U_h^n(\mathbf{x})\}_{n=0}^N \subset H_0(\Omega)$ is called a set of CSLDG numerical solutions to the linear scalar transport equation (1.1) under periodic boundary conditions or compact-support constraints if, for all $\Omega_{\mathcal{K}} \in \mathcal{T}_h$, the following holds:*

$$\int_{\Omega_{\mathcal{K}}} U_{\mathcal{K}}^{n+1}\Psi^{(\mathcal{K})}\,\mathrm{d}\mathbf{x} = \int_{\widetilde{\Omega}_{\mathcal{K}}^{n+1,n}} \widetilde{U}_{\mathcal{K}}^n \psi_{\mathcal{K}}^n(\mathbf{x}; \Psi^{(\mathcal{K})})\,\mathrm{d}\mathbf{x}, \quad \forall \Psi^{(\mathcal{K})} \in H_0(\Omega_{\mathcal{K}}). \tag{2.33}$$

Here, ψ^n is the shorthand notation of $\psi(\mathbf{x}, t_n)$ and $\psi(\mathbf{x}, t_{n+1}) = \Psi$, which satisfies

$$\psi^n(\mathbf{x}) = \Phi_{t_{n+1}\to t_n}^{\mathbf{A}}[\Psi](\mathbf{x}). \tag{2.34}$$

"$\mathcal{K}$", the subscript of ψ and the superscript of Ψ, indicates that the discussion is currently focused on a specific element $\Omega_{\mathcal{K}}$ within the partition $\mathcal{T}_h$ (which is consistent with the intrinsic nature of discontinuous finite elements). This also implies that $\mathrm{supp}\{\Psi^{(\mathcal{K})}\} \subset\subset \Omega_{\mathcal{K}}$. *Clearly,*

$\operatorname{supp}\{\psi_{\mathcal{K}}^n\}$ *is also closely related to* $\Omega_{\mathcal{K}}$. *Lemma 3.1 in the subsequent text will provide further details on this result.*

Remark 2.4. *The definition of the CSLDG numerical solution above avoids dealing with the Cauchy final-value problem for the adjoint equation (1.2) and instead directly defines the relationship between* ψ *and* Ψ *in (2.34). Consequently, the regularity requirement for* Ψ *can be relaxed to* $H_0(\Omega)$ *rather than the* $C_0^1\left(\overline{\Omega}\right)$ *space required in the Cauchy final-value problem*[18]. *"The test function belonging to the lower-regularity H space" aligns more naturally with the conventions of finite element solutions.*

2.3. **Algorithms.**

In this subsection, we focus on the one-dimensional case, i.e., setting $\mathbb{R}^d = \mathbb{R}$ in Equation (1.1), to introduce a specific implementation scheme of the CSLDG algorithm denoted as 1D-CSLDG-A1 [1]. Another existed implementation approach denoted as 1D-CSLDG-A2 can be found in [3]. For the two-dimensional algorithm, please refer to [3, 9, 10].

The one-dimensional form of the integral invariant model is given by:

$$\underbrace{\int_{I_j} u_j^{n+1}(x)\Psi^{(j)}(x)\,\mathrm{d}x}_{LHS_j} = \underbrace{\int_{\tilde{I}_j^{n+1,n}} \tilde{u}_j^n\left(x\right)\psi_j^n\left(x;\Psi^{(j)}\right)\,\mathrm{d}x}_{RHS_j}. \tag{2.35}$$

The pre-determined grid partition $\mathcal{T}_h$ before the computation begins is referred to as the Eulerian grid or background grid (e.g., I_j), which remains unchanged over time. The grid cells obtained by tracing back along the characteristic lines from the Eulerian grid are called Lagrangian grids (e.g., $\tilde{I}_j^{n+1,n}$, hereafter abbreviated as $\tilde{I}_j^\star$). The field function $u(x,t)$ over I_j at t^{n+1} to be solved is approximated by a P-th order DG polynomial, i.e.,

$$u_j^{n+1} = \sum_{m=0}^{P} \alpha_m^{(j)}(t_{n+1})\phi_m^{(j)}(x), \tag{2.36}$$

where $\{\phi_m^{(j)}(x)\}_{m=0}^P$ is a set of orthonormal basis functions (In this paper, we adopt Legendre orthonormal polynomials). By setting $\Psi^{(j)} = \phi_m^{(j)}$, we obtain $LHS_j = \alpha_m^{(j)}(t_{n+1})$. Thus, the key to discrete computation lies in the numerical integration of $RHS_j = \int_{\tilde{I}_j^\star} \tilde{u}_j^n(x)\psi_j^n\left(x;\Psi^{(j)}\right)\,\mathrm{d}x$.

The function $\tilde{u}_j^n$ on the Lagrangian cell $\tilde{I}_j^\star$ can be obtained according to equations (2.11), (2.23), and (2.24). Therefore, the remaining task is to determine how to incorporate the unknown ψ_j^n into the numerical integration process. First, from equation (2.11), it is clear that RHS_j is computed through piecewise integration. Second, in the adjoint problem, the values of ψ along the same characteristic line are constant, which allows us to obtain the ψ function values needed for the numerical integration formula or the interpolation process. Below, we introduce the detailed algorithmic procedures for 1D-CSLDG-A1:

- Step1. Trace the two endpoints $x_{j,L}$ and $x_{j,R}$ of the Eulerian grid I_j at the t_{n+1} layer back to the t_n layer using the characteristic line equation of the adjoint problem:
$$\begin{cases} \frac{dx}{dt} = A(x,t) \\ x(t_{n+1}) = x_{j,L(R)} \end{cases}$$
to obtain the two endpoints $x_{j^\star}^L$ and $x_{j^\star}^R$ of the Lagrangian grid $I_j^\star$.
- Step2. Determine the subintervals $\left\{I_{j,k}^\star\right\}$ of the Lagrangian grid $I_j^\star$ at the t_n layer partitioned by the Eulerian grid based on $x_{j^\star}^L$ and $x_{j^\star}^R$. It is required to identify the Eulerian cell index corresponding to each Lagrangian subinterval at the t_n layer as well as the left and right endpoints $x_{j^\star,k}^R$ and $x_{j^\star,k}^L$ of each Lagrangian subinterval.
- Step3. Place Gaussian quadrature points $\left\{x_{j^\star,k}^g\right\}$ within each subinterval $I_{j,k}^\star$ of the Lagrangian grid $I_j^\star$ at the t_n layer. Note that Gaussian points are generated separately for each subinterval $I_{j,k}^\star$, not for the entire $I_j^\star$.
- Step4. Trace the Gaussian points $\left\{x_{j^\star,k}^g\right\}$ in the subinterval $I_{j,k}^\star$ to the t_{n+1} layer using:
$$\begin{cases} \frac{dx}{dt} = A(x,t) \\ x\left(t_n\right) = x_{j^\star,k}^g \end{cases}$$
to obtain $\left\{x_{j,k}^{n+1,g}\right\}$.
- Step5. Set $\Psi^{(j)}(x) = \phi_m^{(j)}(x)$, where $m = 0, 1, 2, \cdots, P$ (P is the highest degree of the piecewise polynomial). Then, $\psi_j^n\left(x_{j^\star,k}^g\right) = \phi_m^{(j)}\left(x_{j,k}^{n+1,g}\right)$.
- Step6. Compute RHS_j:
$$RHS_j \approx \sum_k \sum_g \frac{\left|x_{j^\star,k}^R - x_{j^\star,k}^L\right|}{2} \cdot w_g \cdot \tilde{u}_{j,k}^n\left(x_{j^\star,k}^g\right) \cdot \phi_m^{(j)}\left(x_{j,k}^{n+1,g}\right).$$

3. Analysis on Fully Discrete Scheme

3.1. **Some Useful Lemmas.**

Note that in the following lemmas, we maintain the assumptions that $\mathbf{A}(\mathbf{x},t)$ has **continuous first-order partial derivatives** and satisfies the **uniformly bounded gradient condition** (2.1). Additionally, please pay attention to the **uniformly bounded divergence** as described in Eq.(2.3):

$$|\nabla_{\mathbf{x}} \cdot \mathbf{A}(\mathbf{x},t)| \le M_A, \ \forall \mathbf{x} \in \mathbb{R}^d, t \in [0,T].$$

Lemma 3.1 (Support of the Time-Dependent Test Function ψ)**.** *Let $\Omega \subset \mathbb{R}^d$ be a bounded domain, and assume* $\operatorname{supp}\{\Psi(x)\} \subset\subset \Omega$. *Let $\psi(\mathbf{x},t)$ satisfy*

$$\psi(\mathbf{x},t) = \Phi_{T\to t}^{\mathbf{A}}[\Psi](\mathbf{x}), \ \forall t \in [0,T].$$

Then, it holds that

$$\operatorname{supp}\{\psi(\mathbf{x},t)\} = \overline{\left\{\mathbf{x} : \ \mathbf{x} + \int_t^T \mathbf{A}(\mathbf{s}(\tau),\tau)\,\mathrm{d}\tau \in \operatorname{supp}\{\Psi\}\right\}}.$$

Let $\widetilde{\Omega}^t = \mathrm{D}^{\mathbf{A}}_{T\to t}(\Omega)$. *Then,* $\mathrm{supp}\{\psi(\mathbf{x},t)\} \subset\subset \widetilde{\Omega}^t$.

Proof.

- For all $\mathbf{x}^* \in \mathrm{supp}\{\psi(\mathbf{x},t)\}$, we have $\psi(\mathbf{x}^*,t) \neq 0$. Consequently, $\Psi\left(\mathbf{x}^* + \int_t^T \mathbf{A}(\mathbf{s}(\tau),\tau)\,\mathrm{d}\tau\right) \neq 0$, which implies $\mathbf{x}^* + \int_t^T \mathbf{A}(\mathbf{s}(\tau),\tau)\,\mathrm{d}\tau \in \mathrm{supp}\{\Psi\}$. Therefore, $\mathbf{x}^* \in \overline{\left\{\mathbf{x} : \mathbf{x} + \int_t^T \mathbf{A}(\mathbf{s}(\tau),\tau)\,\mathrm{d}\tau \in \mathrm{supp}\{\Psi\}\right\}}$. In other words, if $\mathbf{x}^* \in \mathrm{supp}\{\psi(\mathbf{x},t)\}$, then $\mathbf{x}^* \in \overline{\left\{\mathbf{x} : \mathbf{x} + \int_t^T \mathbf{A}(\mathbf{s}(\tau),\tau)\,\mathrm{d}\tau \in \mathrm{supp}\{\Psi\}\right\}}$.
- For all $\mathbf{x}_* \in \overline{\left\{\mathbf{x} : \mathbf{x} + \int_t^T \mathbf{A}(\mathbf{s}(\tau),\tau)\,\mathrm{d}\tau \in \mathrm{supp}\{\Psi\}\right\}}$, we have $\mathbf{x}_* + \int_t^T \mathbf{A}(\mathbf{s}(\tau),\tau)\,\mathrm{d}\tau \in \mathrm{supp}\{\Psi\}$. This implies $\Psi\left(\mathbf{x}_* + \int_t^T \mathbf{A}(\mathbf{s}(\tau),\tau)\,\mathrm{d}\tau\right) \neq 0$, and thus $\psi(\mathbf{x}_*,t) \neq 0$. Consequently, $\mathbf{x}_* \in \mathrm{supp}\{\psi(\mathbf{x},t)\}$. In other words, if $\mathbf{x}_* \in \overline{\left\{\mathbf{x} : \mathbf{x} + \int_t^T \mathbf{A}(\mathbf{s}(\tau),\tau)\,\mathrm{d}\tau \in \mathrm{supp}\{\Psi\}\right\}}$, then $\mathbf{x}_* \in \mathrm{supp}\{\psi(\mathbf{x},t)\}$.

In summary,

$$\mathrm{supp}\{\psi(\mathbf{x},t)\} = \overline{\left\{\mathbf{x} : \mathbf{x} + \int_t^T \mathbf{A}(\mathbf{s}(\tau),\tau)\,\mathrm{d}\tau \in \mathrm{supp}\{\Psi\}\right\}}.$$

Let $\widetilde{\Omega}^t = \mathrm{D}^{\mathbf{A}}_{T\to t}(\Omega)$. By the definition of $\mathrm{D}^{\mathbf{A}}_{T\to t}(\cdot)$, it is clear that $\mathrm{supp}\{\psi(\mathbf{x},t)\} \subset\subset \widetilde{\Omega}^t$. □

Remark 3.1. Ψ *depends only on* $\mathbf{x}$ *and is independent of time* t. *By treating* t *as a fixed time instant, we fix* $\psi(\mathbf{x},t)$ *to be a function of* $\mathbf{x}$ *alone, denoted as* $\psi(\mathbf{x};t)$. *Consequently,* $\mathrm{supp}\{\psi(\mathbf{x};t)\}$ *becomes a set, while being defined with respect to* $\mathbf{x}$*, is contingent upon the chosen value of the parameter* t.

Lemma 3.1 establishes that the time-dependent test function ψ maintains **compact-support** throughout its evolution, and the evolution of its support precisely aligns with the movement and deformation of $\widetilde{\Omega}(t)$.

Lemma 3.2 ($L^P(1 \le P < \infty)$-Norm Control of Time-Dependent Test Functions ψ on Moving Deforming Domains $\widetilde{\Omega}^t$ or Whole Space $\mathbb{R}^d$ Across Time)**.** *Let* $1 \le p < \infty$, *and let* $\Psi \in L^p(\mathcal{G}_T)$, *where the domain* $\mathcal{G}_T$ *is either a bounded domain* $\Omega \subset \mathbb{R}^d$ *or the entire space* $\mathbb{R}^d$. *For any* $t \in [0,T]$, *define the time-evolved domain* $\mathcal{G}_t$ *and the function* $\psi(\cdot,t)$ *via the flow mapping and evolution operator respectively:*

$$\mathcal{G}_t = \mathrm{D}^{\mathbf{A}}_{T\to t}(\mathcal{G}_T); \quad \psi(\mathbf{x},t) = \Phi^{\mathbf{A}}_{T\to t}[\Psi](\mathbf{x}),\ \mathbf{x} \in \mathcal{G}_t.$$

Then, the following norm equivalence holds uniformly in time:

$$e^{-M_A|T-t|/p}\,\|\Psi\|_{L^p(\mathcal{G}_T)} \le \|\psi(\cdot,t)\|_{L^p(\mathcal{G}_t)} \le e^{M_A|T-t|/p}\,\|\Psi\|_{L^p(\mathcal{G}_T)}, \quad \forall t \in [0,T],$$

where the constant M_A *is the uniform bound on the divergence of* $\mathbf{A}$ *as given in the assumption* (2.3).

Proof. It is clear that

$$\|\psi(\cdot\,,t)\|^P_{L^P(\mathcal{G}_t)} = \int_{\mathcal{G}_t} |\psi(\mathbf{x}_t,t)|^P \,\mathrm{d}\mathbf{x}_t = \int_{\mathcal{G}_t} \left|\Phi^{\mathbf{A}}_{T\to t}[\Psi](\mathbf{x}_t)\right|^P \mathrm{d}\mathbf{x}_t = \int_{\mathcal{G}_t} \left|\Psi(\mathrm{D}^{\mathbf{A}}_{t\to T}(\mathbf{x}_t))\right|^P \mathrm{d}\mathbf{x}_t.$$

Perform the following change of variables:

$$\mathbf{x}_T := \mathrm{D}^{\mathbf{A}}_{t\to T}(\mathbf{x}_t)$$

with the corresponding transformations:

$$\mathcal{G}_t \mapsto \mathcal{G}_T.$$

Given that the flow map $\mathrm{D}^{\mathbf{A}}_{t\to T}$ is invertible with inverse $\mathrm{D}^{\mathbf{A}}_{T\to t}$, we have:

$$\mathbf{x}_t = \left(\mathrm{D}^{\mathbf{A}}_{t\to T}\right)^{-1}(\mathbf{x}_T) = \mathrm{D}^{\mathbf{A}}_{T\to t}(\mathbf{x}_T),$$
$$\mathrm{d}\mathbf{x}_t = \left|\det J_{\mathrm{D}^{\mathbf{A}}_{T\to t}}(\mathbf{x}_T)\right| \mathrm{d}\mathbf{x}_T,$$

where $J_{\mathrm{D}^{\mathbf{A}}_{T\to t}}(\mathbf{x}_T)$ is the Jacobian matrix of the flow map $\mathrm{D}^{\mathbf{A}}_{T\to t}$. Then

$$\|\psi(\cdot\,,t)\|^P_{L^P(\mathcal{G}_t)} = \int_{\mathcal{G}_T} |\Psi(\mathbf{x}_T)|^P \left|\det J_{\mathrm{D}^{\mathbf{A}}_{T\to t}}(\mathbf{x}_T)\right| \mathrm{d}\mathbf{x}_T.$$

Noting the definition (Eq.(2.4)) of the reversible flow map $\mathrm{D}^{\mathbf{A}}_{T\to t}$, an application of **Liouville's Formula** [19] yields

$$\left|\det J_{\mathrm{D}^{\mathbf{A}}_{T\to t}}(\mathbf{x}_T)\right| = \left|\det J_{\mathrm{D}^{\mathbf{A}}_{t\to T}}(\mathbf{x}_t)\right|^{-1} = \exp\left(\int_t^T \nabla\cdot\mathbf{A}(\mathbf{s}(\tau),\tau)d\tau\right)^{-1} = \exp\left(-\int_t^T \nabla\cdot\mathbf{A}(\mathbf{s}(\tau),\tau)d\tau\right).$$

Utilizing the **uniformly bounded divergence condition** (Eq. (2.3)), we obtain the following estimate:

$$\exp(-M_A|T-t|) \le \left|\det J_{\mathrm{D}^{\mathbf{A}}_{T\to t}}(\mathbf{x}_T)\right| \le \exp(M_A|T-t|).$$

Consequently,

$$e^{-M_A|T-t|}\int_{\mathcal{G}_T} |\Psi(\mathbf{x}_T)|^P \,\mathrm{d}\mathbf{x}_T \le \int_{\mathcal{G}_T} |\Psi(\mathbf{x}_T)|^P \left|\det J_{\mathrm{D}^{\mathbf{A}}_{T\to t}}(\mathbf{x}_T)\right| \mathrm{d}\mathbf{x}_T \le e^{M_A|T-t|}\int_{\mathcal{G}_T} |\Psi(\mathbf{x}_T)|^P \,\mathrm{d}\mathbf{x}_T,$$

and thus

$$e^{-M_A|T-t|/P}\|\Psi(\cdot\,;T)\|_{L^P(\mathcal{G}_T)} \le \|\psi(\cdot\,,t)\|_{L^P(\mathcal{G}_t)} \le e^{M_A|T-t|/P}\|\Psi(\cdot\,;T)\|_{L^P(\mathcal{G}_T)},\ 1\le P<\infty.$$

□

Remark 3.2. *When $\mathcal{G}_T = \Omega \subset \mathbb{R}^d$, $D^{\mathbf{A}}_{T\to t}(\mathcal{G}_T) = \widetilde{\Omega}(t)$; When $\mathcal{G}_T = \Omega \subset \mathbb{R}^d$, $D^{\mathbf{A}}_{T\to t}(\mathcal{G}_T) = \mathbb{R}^d$.*

Remark 3.3. *Note that in each time step $t_n \to t_{n+1}$ $(n = 0, 1, 2, \ldots, N-1)$ of the CSLDG numerical algorithm, the regular fixed Eulerian background grids $\Omega_{\mathcal{K}}$ and the prescribed test functions $\Psi^{(\mathcal{K})}$ are both placed at the t_{n+1} level. They are then traced back to the t_n level via the characteristic equation $\frac{\mathrm{d}\mathbf{x}}{\mathrm{d}t} = \mathbf{A}(\mathbf{x},t)$ to obtain the upstream Lagrangian cells $\widetilde{\Omega}^{n+1,n}_{\mathcal{K}}$ and the corresponding test functions $\psi^n_{\mathcal{K}}$. Comparing this procedure with Lemma 3.2, we see that in each $t_n \to t_{n+1}$ step, t_{n+1} plays the role of T in Lemma 3.2, while t_n corresponds to*

$t = 0$. This is precisely how the lemma is correctly applied in the subsequent theorem proofs: by setting $T = t_{n+1}$ and $t = t_n$, we obtain $|T - t| = \Delta t$. Since we will be working in the L^2-norm throughout, we take $P = 2$.

When $\nabla \cdot \mathbf{A} = 0$(incompressible flow), M_A diminishes to 0 and the inequalities in Lemma 3.2 become strict equalities. Note that in Lemma 3.2, the control factor $e^{\pm M_A|T-t|/P}$ is **global** and **independent of** $\mathcal{G}_t$, ensuring that the inequalities remain valid even when considering the entire space $\mathbb{R}^d$ with infinite Lebesgue measure. In fact, this factor can be conservatively bounded by $e^{\pm M_A T/P}$, making the control relationship **time-independent**. This lemma form the foundation for key estimates in subsequent proofs.

Lemma 3.3 (Bounded Linear Functional on $H(\mathbb{R}^d)$)**.** *Assume $\mathfrak{U} \in L^2(\mathbb{R}^d)$, $t_p \in [0, T)$, $\Delta t > 0$ and satisfies $t_p + \Delta t \in (0, T]$. For any $W \in H(\mathbb{R}^d)$, define the functional f as follows:*

$$
\begin{aligned}
&f: \ H(\mathbb{R}^d) \longrightarrow \mathbb{R},\\
&f(W; \mathfrak{U}, \mathbf{A}, t_p, \Delta t) = \int_{\mathbb{R}^d} \mathfrak{U} \cdot V(\mathbf{x}; W, \mathbf{A}, t_p, \Delta t)\, \mathrm{d}\mathbf{x},\\
&V(\mathbf{x}; W, \mathbf{A}, t_p, \Delta t) = W\left(\mathbf{x} + \int_{t_p}^{t_p+\Delta t} \mathbf{A}(\mathbf{s}(\tau), \tau)\, \mathrm{d}\tau\right),
\end{aligned}
$$

where $\frac{\mathrm{d}\mathbf{s}}{\mathrm{d}\tau} = \mathbf{A}(\mathbf{s}, \tau)$ with $\mathbf{s}(t_p) = \mathbf{x}$. Then, $\boxed{f \in H^*(\mathbb{R}^d)}$, i.e., f is a bounded linear operator on $H(\mathbb{R}^d)$.

Proof.

- **Linearity**: For all $\phi, \varphi \in H(\mathbb{R}^d)$ and $\lambda, \mu \in \mathbb{R}$,

$$
\begin{aligned}
f(\lambda\phi + \mu\varphi; \mathfrak{U}, \mathbf{A}, t_p, \Delta t) &= \int_{\mathbb{R}^d} \mathfrak{U} \cdot V(\mathbf{x}; \lambda\phi + \mu\varphi, \mathbf{A}, t_p, \Delta t)\, \mathrm{d}\mathbf{x}\\
&= \int_{\mathbb{R}^d} \mathfrak{U} \cdot (\lambda\phi + \mu\varphi)\left(\mathbf{x} + \int_{t_p}^{t_p+\Delta t} \mathbf{A}(\mathbf{s}(\tau), \tau)\, \mathrm{d}\tau\right) \mathrm{d}\mathbf{x}\\
(H(\mathbb{R}^d) \text{ is a linear space}) &= \int_{\mathbb{R}^d} \mathfrak{U} \cdot \left(\lambda\phi\left(\mathbf{x} + \int_{t_p}^{t_p+\Delta t} \mathbf{A}(\mathbf{s}(\tau), \tau)\, \mathrm{d}\tau\right) + \mu\varphi\left(\mathbf{x} + \int_{t_p}^{t_p+\Delta t} \mathbf{A}(\mathbf{s}(\tau), \tau)\, \mathrm{d}\tau\right)\right) \mathrm{d}\mathbf{x}\\
&= \lambda \int_{\mathbb{R}^d} \mathfrak{U} \cdot \phi\left(\mathbf{x} + \int_{t_p}^{t_p+\Delta t} \mathbf{A}(\mathbf{s}(\tau), \tau)\, \mathrm{d}\tau\right) \mathrm{d}\mathbf{x} + \mu \int_{\mathbb{R}^d} \mathfrak{U} \cdot \varphi\left(\mathbf{x} + \int_{t_p}^{t_p+\Delta t} \mathbf{A}(\mathbf{s}(\tau), \tau)\, \mathrm{d}\tau\right) \mathrm{d}\mathbf{x}\\
&= \lambda f(\phi; \mathfrak{U}, \mathbf{A}, t_p, \Delta t) + \mu f(\varphi; \mathfrak{U}, \mathbf{A}, t_p, \Delta t).
\end{aligned}
$$

- **Boundedness (Continuity)**: For all $W \in H(\mathbb{R}^d)$,

$$
\begin{aligned}
|f(W; \mathfrak{U}, \mathbf{A}, t_p, \Delta t)| &\le \int_{\mathbb{R}^d} |\mathfrak{U} \cdot V(\mathbf{x}; W, \mathbf{A}, t_p, \Delta t)|\, \mathrm{d}\mathbf{x}\\
&\le \|\mathfrak{U}\|_{L^2(\mathbb{R}^d)} \cdot \|V(\mathbf{x}; W, \mathbf{A}, t_p, \Delta t)\|_{L^2(\mathbb{R}^d)}\\
(\text{Lemma 3.2}) &\le \|\mathfrak{U}\|_{L^2(\mathbb{R}^d)} \cdot e^{M_A \Delta t} \|W\|_{L^2(\mathbb{R}^d)}\\
&\le e^{M_A T} \|\mathfrak{U}\|_{L^2(\mathbb{R}^d)} \cdot \|W\|_{L^2(\mathbb{R}^d)}.
\end{aligned}
$$

□

Lemma 3.3 establishes the foundation for applying the Riesz Representation Theorem in the subsequent existence proof.

Lemma 3.4 (Norm control under extension between bounded domains)**.** *Let $\Omega_1, \Omega_2 \subset \mathbb{R}^d$ be two bounded domains. For any function $v \in L^2(\Omega_1)$, define $\widetilde{v}$ as the function obtained by extending v to Ω_2 in the following manner:*

- *For zero extension (compact support case): $\widetilde{v}(\mathbf{x}) = v(\mathbf{x})$ if $\mathbf{x} \in \Omega_1 \cap \Omega_2$, and $\widetilde{v}(\mathbf{x}) = 0$ otherwise.*
- *For periodic extension (periodic boundary condition case): assume Ω_1 is a fundamental cell, and $\widetilde{v}$ is obtained by periodically replicating v to cover Ω_2, then restricting to Ω_2.*

Then there exists a constant E, depending only on Ω_1, Ω_2 and the type of extension, such that

$$\|\widetilde{v}\|_{L^2(\Omega_2)} \leq E\|v\|_{L^2(\Omega_1)} \quad \forall v \in L^2(\Omega_1).$$

The constant E is independent of v.

Proof. For zero extension, we have

$$\|\widetilde{v}\|^2_{L^2(\Omega_2)} = \int_{\Omega_1 \cap \Omega_2} |v|^2 \, d\mathbf{x} \leq \int_{\Omega_1} |v|^2 \, d\mathbf{x} = \|v\|^2_{L^2(\Omega_1)},$$

so $E = 1$ suffices.

For periodic extension, Ω_2 can be covered by at most N (complete or partial) copies of the fundamental cell Ω_1, where N depends only on the relative sizes of Ω_2 and Ω_1. Then

$$\|\widetilde{v}\|^2_{L^2(\Omega_2)} \leq N\|v\|^2_{L^2(\Omega_1)},$$

and we may take $E = \sqrt{N}$. □

Remark 3.4. *If a mesh partition $\mathcal{T}_h^d$ is introduced on the bounded domain Ω, it is evident that the extension control constant E in this lemma is independent of h. The constants C_i appearing in the proof of the stability theorem 3.2, are precisely instances of this extension control constant corresponding to the domains Ω and $\widetilde{\Omega}^{i+1,i}$. Consequently, their maxima — C in Theorem 3.2 — depend only on $(T, \Delta t, \Omega, \mathbf{A})$ and are independent of h ($(T, \Delta t, \Omega, \mathbf{A})$ influences the relative sizes of Ω and $\widetilde{\Omega}^{i+1,i}$, thereby affecting the extension control constants).*

3.2. **Existence, Stability and Uniqueness for CSLDG Numerical Solutions.**

All the conclusions in this subsection hold under both periodic boundary conditions and compact-support boundary conditions. The proof is only carried out under the compact-support boundary conditions. For periodic boundary conditions, simply replace "the whole space $\mathbb{R}^d$" with $\widehat{\Omega}$ in the proof process below (the definition of $\widehat{\Omega}$ can be found in Eq. (2.30)).

Note that

$$\text{Compact support:}\quad \Omega \xrightarrow[\text{zero extension}]{} \widetilde{\Omega}(t) \xrightarrow[\text{zero extension}]{} \mathbb{R}^d;$$

$$\text{Periodic boundary:}\quad \Omega \xrightarrow{\text{periodic extension}} \widetilde{\Omega}(t) \xrightarrow{\text{zero extension}} \widehat{\Omega}.$$

The following three propositions and their proofs all involve the definition of U_i^n (specifically, the relationship between U_i^n and U_h^n). Please consistently refer to Equations (2.17) through (2.20) in the preceding text.

Proposition 3.1. *Let $\mathcal{T}_h = \bigcup_{i=1}^M \Omega_i$ be a spatial partition of a bounded domain Ω. If $U_h^n \in L^2(\Omega)$, then $U_i^n \in L^2(\Omega_i)$ for all $\Omega_i \in \mathcal{T}_h$. Conversely, the same holds.*

Proof.

Noting that $U_i^n = U_h^n \cdot \chi_{\Omega_i}(\mathbf{x})$, if $U_h^n \in L^2(\Omega)$, then

$$\infty > \int_\Omega |U_h^n|^2 \,\mathrm{d}\mathbf{x} = \sum_{\Omega_k \in \mathcal{T}_h} \int_{\Omega_k} |U_h^n|^2 \,\mathrm{d}\mathbf{x} \geq \int_{\Omega_i} |U_h^n|^2 \,\mathrm{d}\mathbf{x} = \int_{\Omega_i} |U_i^n|^2 \,\mathrm{d}\mathbf{x}.$$

Conversely, if $U_i^n \in L^2(\Omega_i)$ for all $\Omega_i \in \mathcal{T}_h$, then

$$\int_\Omega |U_h^n|^2 \,\mathrm{d}\mathbf{x} = \sum_{\Omega_i \in \mathcal{T}_h} \int_{\Omega_i} |U_h^n|^2 \,\mathrm{d}\mathbf{x} = \sum_{\Omega_i \in \mathcal{T}_h} \int_{\Omega_i} |U_i^n|^2 \,\mathrm{d}\mathbf{x} < \infty.$$

□

Proposition 3.2. *Let $\mathcal{T}_h = \bigcup_{i=1}^M \Omega_i$ be a spatial partition of the bounded domain Ω. If $U_h^n \in L^2(\mathbb{R}^d)$, noting $\mathrm{supp}\{U_i^n\} \subset\subset \Omega_i$, we have $U_i^n \in H_0(\Omega_i)$ for all $\Omega_i \in \mathcal{T}_h$. Conversely, if $U_i^n \in H_0(\Omega_i)$ for all $\Omega_i \in \mathcal{T}_h$, then $U_h^n \in H_0(\Omega)$.*

Proof.

From equations (2.17) to (2.20), it is known that $\mathrm{supp}\{U_i^n\} \subset\subset \Omega_i$, $\mathrm{supp}\{U_h^n\} \subset\subset \Omega$. Therefore, if $U_h^n \in L^2(\mathbb{R}^d)$, then $U_h^n \in H_0(\Omega)$, and we have

$$\begin{aligned}\infty > \int_{\mathbb{R}^d} |U_h^n|^2 \,\mathrm{d}\mathbf{x} &= \int_\Omega |U_h^n|^2 \,\mathrm{d}\mathbf{x} + \int_{\mathbb{R}^d\setminus\Omega} |U_h^n|^2 \,\mathrm{d}\mathbf{x} = \int_\Omega |U_h^n|^2 \,\mathrm{d}\mathbf{x} + \int_{\mathbb{R}^d\setminus\Omega} |0|^2 \,\mathrm{d}\mathbf{x} \\ &= \sum_{\Omega_k \in \mathcal{T}_h} \int_{\Omega_k} |U_h^n|^2 \,\mathrm{d}\mathbf{x} = \sum_{\Omega_k \in \mathcal{T}_h} \int_{\Omega_k} |U_k^n|^2 \,\mathrm{d}\mathbf{x} \geq \int_{\Omega_i} |U_i^n|^2 \,\mathrm{d}\mathbf{x},\end{aligned}$$

which implies $U_i^n \in L^2(\Omega_i)$. Since $\mathrm{supp}\{U_i^n\} \subset\subset \Omega_i$, it further follows that $U_i^n \in H_0(\Omega_i)$. Then $U_i^n \in L^2(\mathbb{R}^d)$ is evident, as shown below:

$$\int_{\mathbb{R}^d} |U_i^n|^2 \,\mathrm{d}\mathbf{x} = \int_{\Omega_i} |U_i^n|^2 \,\mathrm{d}\mathbf{x} + \int_{\mathbb{R}^d\setminus\Omega_i} |U_i^n|^2 \,\mathrm{d}\mathbf{x} = \int_{\Omega_i} |U_i^n|^2 \,\mathrm{d}\mathbf{x} + \int_{\mathbb{R}^d\setminus\Omega_i} |0|^2 \,\mathrm{d}\mathbf{x} = \int_{\Omega_i} |U_i^n|^2 \,\mathrm{d}\mathbf{x} < \infty.$$

Conversely, if $U_i^n \in H_0(\Omega_i)$, then $\mathrm{supp}\{U_i^n\} \subset\subset \Omega_i$ and $U_i^n \in L^2(\Omega_i)$. From $\mathrm{supp}\{U_i^n\} \subset\subset \Omega_i$ and Eq.(2.19), it follows that $\mathrm{supp}\{U_h^n\} \subset\subset \Omega$; from $U_i^n \in L^2(\Omega_i)$ and Proposition 3.1, we deduce $U_h^n \in L^2(\Omega)$. Thus, $U_h^n \in H_0(\Omega)$ (and it is evident that $U_h^n \in L^2(\mathbb{R}^d)$). □

Proposition 3.3. *Let $\mathcal{T}_h = \bigcup_{i=1}^{M} \Omega_i$ be a spatial partition of a bounded domain Ω. If $U_h^n \in L^2(\mathbb{R}^d)$, given that $\mathrm{supp}\{U_i^n\} \subset\subset \Omega_i$, it holds that $\widetilde{U}_{\mathcal{K}}^n \in H_0(\widetilde{\Omega}_{\mathcal{K}}^{n+1,n})$.*

Proof.

If $U_h^n \in L^2(\mathbb{R}^d)$, noting $\mathrm{supp}\{U_i^n\} \subset\subset \Omega_i$, by Proposition 3.2, it follows that

$$U_{\mathcal{K}_i}^n \in H_0(\Omega_{\mathcal{K}_i}), \quad \forall U_{\mathcal{K}_i}^n \in \mathbb{U}(\widetilde{\Omega}_{\mathcal{K}}^{n+1,n}).$$

Since $\left\{\Omega_{\mathcal{K}_i} \cap \widetilde{\Omega}_{\mathcal{K}}^{n+1,n}\right\} \subset \Omega_{\mathcal{K}_i}$, we have

$$\int_{\Omega_{\mathcal{K}_i} \cap \widetilde{\Omega}_{\mathcal{K}}^{n+1,n}} \left|U_{\mathcal{K}_i}^n\right|^2 \, \mathrm{d}\mathbf{x} \leq \int_{\Omega_{\mathcal{K}_i}} \left|U_{\mathcal{K}_i}^n\right|^2 \, \mathrm{d}\mathbf{x} < \infty,$$

which implies $U_{\mathcal{K}_i}^n\big|_{\left\{\Omega_{\mathcal{K}_i} \cap \widetilde{\Omega}_{\mathcal{K}}^{n+1,n}\right\}} \in L^2(\Omega_{\mathcal{K}_i} \cap \widetilde{\Omega}_{\mathcal{K}}^{n+1,n})$. Moreover, Property Eq.(2.13) ensures that $\bigcup_{i=1}^{d_s} \left\{\Omega_{\mathcal{K}_i} \cap \widetilde{\Omega}_{\mathcal{K}}^{n+1,n}\right\}$ is a spatial partition of $\widetilde{\Omega}_{\mathcal{K}}^{n+1,n}$. Consequently, from Proposition 3.1, we obtain $\widetilde{U}_{\mathcal{K}}^n \in L^2(\widetilde{\Omega}_{\mathcal{K}}^{n+1,n})$. Furthermore, from equation (2.25), $\mathrm{supp}\{\widetilde{U}_{\mathcal{K}}^n\} \subset\subset \widetilde{\Omega}_{\mathcal{K}}^{n+1,n}$, and thus $\widetilde{U}_{\mathcal{K}}^n \in H_0(\widetilde{\Omega}_{\mathcal{K}}^{n+1,n})$ (from which $\widetilde{U}_{\mathcal{K}}^n \in L^2(\mathbb{R}^d)$ is trivial). □

Theorem 3.1. *Under compact-support boundary conditions, given the initial value $U_0(\mathbf{x}) \in L^2(\Omega)$, for any time partition $T = N\Delta t$ and any spatial partition $\mathcal{T}_h$, there exists $U_h^n(\mathbf{x}) \in H_0(\Omega)$ $(n = 1, 2, 3, \ldots, N)$ that satisfies the fully discrete scheme (2.33) in Definition 2.1.*

Proof. we employ mathematical induction to prove it:

- For $n = 1$, we aim to prove that for any $\Omega_{\mathcal{K}} \in \mathcal{T}_h$,

$$\exists U_{\mathcal{K}}^1 \in H_0(\Omega_{\mathcal{K}}) \ s.t. \ \int_{\Omega_{\mathcal{K}}} U_{\mathcal{K}}^1 \Psi^{(\mathcal{K})} \, \mathrm{d}\mathbf{x} = \int_{\widetilde{\Omega}_{\mathcal{K}}^{1,0}} \widetilde{U}_{\mathcal{K}}^0 \psi^0(\mathbf{x}; \Psi^{(\mathcal{K})}) \, \mathrm{d}\mathbf{x}, \ \forall \Psi^{(\mathcal{K})} \in H_0(\Omega_{\mathcal{K}}).$$

  Given $U_0 \in L^2(\Omega)$, under the compact-support boundary conditions ($\mathrm{supp}\{U_0\} \subset\subset \Omega$), $U_0 \in L^2(\mathbb{R}^d)$. By Proposition 3.3, we have

$$\widetilde{U}_{\mathcal{K}}^0 \in L^2(\mathbb{R}^d), \quad \forall \Omega_{\mathcal{K}} \in \mathcal{T}_h. \tag{3.1}$$

  $\Psi^{(\mathcal{K})}$ and $\psi_{\mathcal{K}}^0$ satisfy

$$\Psi^{(\mathcal{K})} = \psi_{\mathcal{K}}^0(\mathbf{x} + \int_0^{\Delta t} \mathbf{A}(\mathbf{s}(\tau), \tau) \, \mathrm{d}\tau), \tag{3.2}$$

  so we can write

$$\int_{\Omega_{\mathcal{K}}} U_{\mathcal{K}}^1 \Psi^{(\mathcal{K})} \, \mathrm{d}\mathbf{x} = \int_{\widetilde{\Omega}_{\mathcal{K}}^{1,0}} \widetilde{U}_{\mathcal{K}}^0 \Psi^{(\mathcal{K})} \left(\mathbf{x} + \int_0^{\Delta t} \mathbf{A}(\mathbf{s}(\tau), \tau) \, \mathrm{d}\tau\right) \mathrm{d}\mathbf{x} = \int_{\widetilde{\Omega}_{\mathcal{K}}^{1,0}} \widetilde{U}_{\mathcal{K}}^0 \psi_{\mathcal{K}}^0(\mathbf{x}; \Psi^{(\mathcal{K})}, \mathbf{A}, 0, \Delta t) \, \mathrm{d}\mathbf{x}. \tag{3.3}$$

  Introducing the functional $f^{1,0}(\omega; \widetilde{U}_{\mathcal{K}}^0, \mathbf{A}, 0, \Delta t) = \int_{\mathbb{R}^d} \widetilde{U}_{\mathcal{K}}^0 \psi_{\mathcal{K}}^0(\mathbf{x}; \Psi^{(\mathcal{K})}, \mathbf{A}, 0, \Delta t) \, \mathrm{d}\mathbf{x}$, for $\omega \in H(\mathbb{R}^d)$, by Lemma 3.3, we know $f^{1,0} \in H^*(\mathbb{R}^d)$. Therefore, by the "Riesz Representation Theorem", for all $w \in H(\mathbb{R}^d)$, there exists a unique $\mathcal{W}_{\mathcal{K}}^1 \in H(\mathbb{R}^d)$ such that

$$\langle \mathcal{W}_{\mathcal{K}}^1, w \rangle_{L^2(\mathbb{R}^d)} = f^{1,0}(w; \widetilde{U}_{\mathcal{K}}^0, \mathbf{A}, 0, \Delta t). \tag{3.4}$$

Since $\Psi^{(\mathcal{K})} \in H_0(\Omega_{\mathcal{K}}) \subset H(\mathbb{R}^d)$, we have

$$\langle \mathcal{W}^1_{\mathcal{K}}, \Psi^{(\mathcal{K})} \rangle_{L^2(\mathbb{R}^d)} = f^{1,0}(\Psi^{(\mathcal{K})}; \widetilde{U}^0_{\mathcal{K}}, \mathbf{A}, 0, \Delta t), \quad \forall \Psi^{(\mathcal{K})} \in H_0(\Omega_{\mathcal{K}}). \tag{3.5}$$

Noting that
$\mathrm{supp}\{\Psi^{(\mathcal{K})}\} \subset\subset \Omega_{\mathcal{K}}$, we have

$$\langle W^1_{\mathcal{K}}, \Psi^{(\mathcal{K})} \rangle_{L^2(\mathbb{R}^d)} = \langle W^1_{\mathcal{K}}, \Psi^{(\mathcal{K})} \rangle_{L^2(\Omega_{\mathcal{K}})} = \int_{\Omega_{\mathcal{K}}} W^1_{\mathcal{K}} \Psi^{(\mathcal{K})} \, \mathrm{d}\mathbf{x}. \tag{3.6}$$

$\mathrm{supp}\{\psi^0_{\mathcal{K}}\} \subset\subset \widetilde{\Omega}^{1,0}_{\mathcal{K}}$ (by Lemma 3.1), we have

$$f(\Psi^{(\mathcal{K})}; U^0, \mathbf{A}, 0, \Delta t) = \int_{\mathbb{R}^d} U^0 \psi^0_{\mathcal{K}}(\mathbf{x}; \Psi^{(\mathcal{K})}, \mathbf{A}, 0, \Delta t) \, \mathrm{d}\mathbf{x} = \int_{\widetilde{\Omega}^{1,0}_{\mathcal{K}}} U^0 \psi^0_{\mathcal{K}}(\mathbf{x}; \Psi^{(\mathcal{K})}, \mathbf{A}, 0, \Delta t) \, \mathrm{d}\mathbf{x}; \tag{3.7}$$

Thus,

$$\exists! W^1_{\mathcal{K}} \in H(\mathbb{R}^d) \ s.t. \ \int_{\Omega_{\mathcal{K}}} W^1_{\mathcal{K}} \Psi^{(\mathcal{K})} \, \mathrm{d}\mathbf{x} = \int_{\widetilde{\Omega}^{1,0}_{\mathcal{K}}} U^0 \psi^0_{\mathcal{K}}(\mathbf{x}; \Psi^{(\mathcal{K})}, \mathbf{A}, 0, \Delta t) \, \mathrm{d}\mathbf{x}, \ \forall \Psi^{(\mathcal{K})} \in H_0(\Omega_{\mathcal{K}}).$$

We set

$$U^1_{\mathcal{K}}(\mathbf{x}) = W^1_{\mathcal{K}}(\mathbf{x}) \cdot \chi_{\Omega_{\mathcal{K}}}(\mathbf{x}), \tag{3.8}$$

thus, $U^1_{\mathcal{K}} \in H_0(\Omega_{\mathcal{K}}) \subset H(\mathbb{R}^d)$ and

$$\int_{\Omega_{\mathcal{K}}} U^1_{\mathcal{K}} \Psi^{(\mathcal{K})} \, \mathrm{d}\mathbf{x} = \int_{\Omega_{\mathcal{K}}} W^1_{\mathcal{K}} \Psi^{(\mathcal{K})} \, \mathrm{d}\mathbf{x}. \tag{3.9}$$

Therefore,

$$\exists U^1_{\mathcal{K}} \in H_0(\Omega_{\mathcal{K}}) \quad \text{s.t.} \quad \int_{\Omega_{\mathcal{K}}} U^1_{\mathcal{K}} \Psi^{(\mathcal{K})} \, \mathrm{d}\mathbf{x} = \int_{\widetilde{\Omega}^{1,0}_{\mathcal{K}}} U^0 \psi^0_{\mathcal{K}}(\mathbf{x}; \Psi^{(\mathcal{K})}, \mathbf{A}, 0, \Delta t) \, \mathrm{d}\mathbf{x}, \quad \forall \Psi^{(\mathcal{K})} \in H_0(\Omega_{\mathcal{K}}). \tag{3.10}$$

Noting that $\Omega_{\mathcal{K}}$ is an arbitrary element in the spatial partition $\mathcal{T}_h$ of Ω, we can construct

$$U^1_h(\mathbf{x}) = \sum_{\Omega_{\mathcal{K}} \in \mathcal{T}_h} U^1_{\mathcal{K}}(\mathbf{x}), \tag{3.11}$$

which implies $\mathrm{supp}\{U^1_h\} \subset\subset \Omega$ and satisfies

$$U^1_{\mathcal{K}}(\mathbf{x}) = U^1_h(\mathbf{x}) \cdot \chi_{\Omega_{\mathcal{K}}}(\mathbf{x}), \quad \forall \Omega_{\mathcal{K}} \in \mathcal{T}_h. \tag{3.12}$$

Furthermore, by Proposition 3.2, we have

$$U^1_h \in H_0(\Omega). \tag{3.13}$$

Combining Eqs.(3.13)(3.12) and (3.10), we conclude that U^1_h satisfies the fully discrete scheme (2.33) from Definition 2.1.

- Assume that the conclusion holds for $n = m$, i.e.,
  $\exists U_h^n(\mathbf{x}) \in H_0(\Omega) \quad (n = 1, 2, \ldots, m)$ satisfying the fully discrete scheme (2.33).
  We now prove that the conclusion holds for $n = m + 1$:
  At this stage, U_h^m is given, analogous to U_0 in the proof for $n = 1$. Following the same reasoning as in the proof for $n = 1$, we obtain

$$\exists U_{\mathcal{K}}^{m+1} \in H_0(\Omega_{\mathcal{K}}) \; s.t. \int_{\Omega_{\mathcal{K}}} U_{\mathcal{K}}^{m+1} \Psi^{(\mathcal{K})} \, \mathrm{d}\mathbf{x} = \int_{\widetilde{\Omega}_{\mathcal{K}}^{m+1,m}} \widetilde{U}_{\mathcal{K}}^m \psi_{\mathcal{K}}^m(\mathbf{x}; \Psi^{(\mathcal{K})}, \mathbf{A}, t_m, \Delta t) \, \mathrm{d}\mathbf{x}, \; \forall \Psi^{(\mathcal{K})} \in H_0(\Omega_{\mathcal{K}}).$$

  We construct $U_h^{m+1}(\mathbf{x})$ as follows:

$$U_h^{m+1}(\mathbf{x}) = \sum_{\Omega_{\mathcal{K}} \in \mathcal{T}_h} U_{\mathcal{K}}^{m+1}, \tag{3.14}$$

  which implies $\mathrm{supp}\{U_h^{m+1}\} \subset\subset \Omega$ and satisfies

$$U_{\mathcal{K}}^{m+1}(\mathbf{x}) = U_h^{m+1}(\mathbf{x}) \cdot \chi_{\Omega_{\mathcal{K}}}(\mathbf{x}), \quad \forall \Omega_{\mathcal{K}} \in \mathcal{T}_h. \tag{3.15}$$

  By Proposition 3.2, we have

$$U_h^{m+1} \in H_0(\Omega). \tag{3.16}$$

  Clearly, U_h^{m+1} satisfies the fully discrete scheme (2.33).
  Therefore, $\exists U_h^n(\mathbf{x}) \in H_0(\Omega)$ $(n = 1, 2, \ldots, m, m+1)$ that satisfy the fully discrete scheme (2.33).

In summary, Theorem 3.1 is proved. □

Remark 3.5. *The proof of Theorem 3.1 does not establish the uniqueness of U_h^n. Although $\{W_{\mathcal{K}}^n\}_{\mathcal{K}=1}^M$ is unique, the construction of $U_{\mathcal{K}}^n$ and U_h^n based on $\{W_{\mathcal{K}}^n\}_{\mathcal{K}=1}^M$ is not necessarily unique, as indicated by equations (3.8), (3.11), and (3.14). Therefore, we consider demonstrating the uniqueness of U_h^n from the perspective of the continuous dependence of U_h^n on the initial data (stability), as detailed in Theorem 3.3.*

Theorem 3.2. *Under compact-support boundary conditions, for a given initial condition $U_0(\mathbf{x}) \in L^2(\Omega)$, the solution to the fully discrete scheme (2.33) is unconditionally stable and satisfies*

$$\|U^n(\mathbf{x})\|_{L^2(\Omega)} \le C \|U_0(\mathbf{x})\|_{L^2(\Omega)}, \quad n = 1, 2, 3, \ldots, N. \tag{3.17}$$

Here, C is a positive constant depending on $(T, \Delta t, \Omega, \mathbf{A})$.

Proof.

Given the initial value $U_0(\mathbf{x})$ perturbed to $W_0(\mathbf{x})$ with $W_0 \in L^2(\Omega)$, the CSLDG numerical solutions of Eq.(1.1) with initial values U_0 and W_0 are denoted by U_h^n and W_h^n $(n = 1, 2, \ldots, N)$, respectively. Thus, for all $\Omega_{\mathcal{K}} \in \mathcal{T}_h$, we have

$$\int_{\Omega_{\mathcal{K}}} U_{\mathcal{K}}^{n+1} \cdot \Psi^{(\mathcal{K})} \, \mathrm{d}\mathbf{x} = \int_{\widetilde{\Omega}_{\mathcal{K}}^{n+1,n}} \widetilde{U}_{\mathcal{K}}^n \cdot \psi_{\mathcal{K}}^n(\mathbf{x}; \Psi^{(\mathcal{K})}) \, \mathrm{d}\mathbf{x}, \; \forall \Psi^{(\mathcal{K})} \in H_0(\Omega_{\mathcal{K}}); \tag{3.18a}$$

$$\int_{\Omega_{\mathcal{K}}} W_{\mathcal{K}}^{n+1} \cdot \Psi^{(\mathcal{K})} \, \mathrm{d}\mathbf{x} = \int_{\widetilde{\Omega}_{\mathcal{K}}^{n+1,n}} \widetilde{W}_{\mathcal{K}}^n \cdot \psi_{\mathcal{K}}^n(\mathbf{x}; \Psi^{(\mathcal{K})}) \, \mathrm{d}\mathbf{x}, \; \forall \Psi^{(\mathcal{K})} \in H_0(\Omega_{\mathcal{K}}). \tag{3.18b}$$

Subtracting Eq. (3.18b) from Eq. (3.18a), we obtain

$$\int_{\Omega_{\mathcal{K}}} \left(U_{\mathcal{K}}^{n+1} - W_{\mathcal{K}}^{n+1}\right) \cdot \Psi^{(\mathcal{K})} \, \mathrm{d}\mathbf{x} = \int_{\widetilde{\Omega}_{\mathcal{K}}^{n+1,n}} \left(\widetilde{U}_{\mathcal{K}}^{n} - \widetilde{W}_{\mathcal{K}}^{n}\right) \cdot \psi_{\mathcal{K}}^{n}(\mathbf{x}; \Psi^{(\mathcal{K})}) \, \mathrm{d}\mathbf{x}, \quad \forall \Psi^{(\mathcal{K})} \in H_0(\Omega_{\mathcal{K}}). \tag{3.19}$$

Taking

$$\Psi^{(\mathcal{K})} = U_{\mathcal{K}}^{n+1} - W_{\mathcal{K}}^{n+1}, \tag{3.20}$$

by Theorem 3.1, we know that $U_h^{n+1}, W_h^{n+1} \in H_0(\Omega)$. Furthermore, by Proposition 3.2, it follows that $U_{\mathcal{K}}^{n+1}, W_{\mathcal{K}}^{n+1} \in H_0(\Omega_{\mathcal{K}})$. Consequently, $\Psi^{(\mathcal{K})} \in H_0(\Omega_{\mathcal{K}})$.
We still proceed with the proof using mathematical induction:

- For $n = 1$,

$$\begin{aligned} \int_{\Omega_{\mathcal{K}}} \left|U_{\mathcal{K}}^{1} - W_{\mathcal{K}}^{1}\right|^2 \mathrm{d}\mathbf{x} &\leq \int_{\widetilde{\Omega}_{\mathcal{K}}^{1,0}} \left|\left(\widetilde{U}_{\mathcal{K}}^{0} - \widetilde{W}_{\mathcal{K}}^{0}\right) \cdot \psi_{\mathcal{K}}^{0}(\mathbf{x}; \Psi^{(\mathcal{K})})\right| \mathrm{d}\mathbf{x} \\ &\leq \|\widetilde{U}_{\mathcal{K}}^{0} - \widetilde{W}_{\mathcal{K}}^{0}\|_{L^2(\widetilde{\Omega}_{\mathcal{K}}^{1,0})} \cdot \|\psi_{\mathcal{K}}^{0}(\mathbf{x}; \Psi^{(\mathcal{K})})\|_{L^2(\widetilde{\Omega}_{\mathcal{K}}^{1,0})}. \end{aligned} \tag{3.21}$$

  Take $P = 2$ in Lemma 3.2, we have

$$\|\psi_{\mathcal{K}}^{0}(\mathbf{x}; \Psi^{(\mathcal{K})})\|_{L^2(\widetilde{\Omega}_{\mathcal{K}}^{1,0})} \leq e^{M_A|t_1 - 0|/2} \|\Psi^{(\mathcal{K})}\|_{L^2(\Omega_{\mathcal{K}})} = e^{M_A \Delta t/2} \|\Psi^{(\mathcal{K})}\|_{L^2(\Omega_{\mathcal{K}})}, \tag{3.22}$$

  and thus,

$$\|\psi_{\mathcal{K}}^{0}(\mathbf{x}; \Psi^{(\mathcal{K})})\|_{L^2(\widetilde{\Omega}_{\mathcal{K}}^{1,0})} \leq e^{M_A \Delta t/2} \|U_{\mathcal{K}}^{1} - W_{\mathcal{K}}^{1}\|_{L^2(\Omega_{\mathcal{K}})}, \tag{3.23}$$

  Therefore,

$$\|U_{\mathcal{K}}^{1} - W_{\mathcal{K}}^{1}\|_{L^2(\Omega_{\mathcal{K}})} \leq e^{M_A \Delta t/2} \|\widetilde{U}_{\mathcal{K}}^{0} - \widetilde{W}_{\mathcal{K}}^{0}\|_{L^2(\widetilde{\Omega}_{\mathcal{K}}^{1,0})}, \ \forall \Omega_{\mathcal{K}} \in \mathcal{T}_h^d. \tag{3.24}$$

  By summing equation (3.24) over all $\Omega_{\mathcal{K}}$ and noting that $\mathrm{supp}\{U_{\mathcal{K}}^{1}\} = \Omega_{\mathcal{K}}, \mathrm{supp}\{W_{\mathcal{K}}^{1}\} = \Omega_{\mathcal{K}}$, we obtain

$$\|U_h^1 - W_h^1\|_{L^2(\Omega)}^2 = \sum_{\mathcal{K}=1}^{M} \|U_{\mathcal{K}}^{1} - W_{\mathcal{K}}^{1}\|_{L^2(\Omega_{\mathcal{K}})}^2 \leq e^{M_A \Delta t/2} \sum_{\mathcal{K}=1}^{M} \|\widetilde{U}_{\mathcal{K}}^{0} - \widetilde{W}_{\mathcal{K}}^{0}\|_{L^2(\widetilde{\Omega}_{\mathcal{K}}^{1,0})}^2, \tag{3.25}$$

  Given that $\mathrm{supp}\{\widetilde{U}_{\mathcal{K}}^{0}\} = \widetilde{\Omega}_{\mathcal{K}}^{1,0}$ and $\mathrm{supp}\{\widetilde{W}_{\mathcal{K}}^{0}\} = \widetilde{\Omega}_{\mathcal{K}}^{1,0}$, it follows analogously that

$$\sum_{\mathcal{K}=1}^{M} \|\widetilde{U}_{\mathcal{K}}^{0} - \widetilde{W}_{\mathcal{K}}^{0}\|_{L^2(\widetilde{\Omega}_{\mathcal{K}}^{1,0})}^2 = \|\widetilde{U}_h^0 - \widetilde{W}_h^0\|_{L^2(\widetilde{\Omega}^{1,0})}^2, \tag{3.26}$$

  Thus, we conclude that

$$\|U_h^1 - W_h^1\|_{L^2(\Omega)}^2 \leq e^{M_A \Delta t/2} \|\widetilde{U}_h^0 - \widetilde{W}_h^0\|_{L^2(\widetilde{\Omega}^{1,0})}^2. \tag{3.27}$$

  Under periodic or compact-support boundary conditions, Lemma 3.4 implies there exists $C_0 > 0$ such that

$$|\widetilde{U}_h^0 - \widetilde{W}_h^0\|_{L^2(\widetilde{\Omega}^{1,0})}^2 \leq C_0 \|U_0 - W_0\|_{L^2(\Omega)}^2, \tag{3.28}$$

Note C_0 is independent of mesh size h. Taking $C = e^{M_A \Delta t/2} C_0 > 0$, we have

$$\|U_h^1 - W_h^1\|_{L^2(\Omega)}^2 \le C \|U_0 - W_0\|_{L^2(\Omega)}^2. \tag{3.29}$$

- Assume that the conclusion holds for $n = k$, i.e.,

$$\|U_h^n - W_h^n\|_{L^2(\Omega)}^2 \le C \|U_0 - W_0\|_{L^2(\Omega)}^2, \quad n = 1, 2, \ldots, k, \tag{3.30}$$

where

$$C = \max\{e^{M_A \Delta t/2} C_0, e^{M_A \cdot 2\Delta t/2} C_1 \cdot C_0, \ldots, e^{M_A \cdot k \Delta t/2} \prod_{i=0}^{k-1} C_i\} > 0$$

and C_i satisfies

$$\|\widetilde{U}_h^i - \widetilde{W}_h^i\|_{L^2(\widetilde{\Omega}^{i+1,i})}^2 \le C_i \|U_h^i - W_h^i\|_{L^2(\Omega)}^2 \ (i = 0, 1, \ldots, k-1).$$

(Under periodic or compact-support boundary conditions, such a constant C_i is guaranteed to exist and independent of h according to Lemma 3.4.)

For $n = k + 1$, following the same reasoning as in the case $n = 1$, we obtain that there exists $C_k > 0$ such that

$$\|U_h^{k+1} - W_h^{k+1}\|_{L^2(\Omega)}^2 \le C_k e^{M_A \Delta t/2} \|U_h^k - W_h^k\|_{L^2(\Omega)}^2. \tag{3.31}$$

Then,

$$\begin{aligned} \|U_h^{k+1} - W_h^{k+1}\|_{L^2(\Omega)}^2 &\le e^{M_A \Delta t/2} C_k \cdot e^{M_A \cdot k \Delta t/2} \prod_{i=0}^{k-1} C_i \|U_0 - W_0\|_{L^2(\Omega)}^2 \\ &= e^{M_A \cdot (k+1) \Delta t/2} \prod_{i=0}^{k} C_i \|U_0 - W_0\|_{L^2(\Omega)}^2. \end{aligned} \tag{3.32}$$

By defining

$$C = \max\{e^{M_A \Delta t/2} C_0, e^{M_A \cdot 2\Delta t/2} C_1 \cdot C_0, \ldots, e^{M_A \cdot k \Delta t/2} \prod_{i=0}^{k-1} C_i, e^{M_A \cdot (k+1) \Delta t/2} \prod_{i=0}^{k} C_i\} > 0,$$

we conclude that

$$\|U_h^n - W_h^n\|_{L^2(\Omega)}^2 \le C \|U_0 - W_0\|_{L^2(\Omega)}^2, \ n = 1, 2, \ldots, k+1. \tag{3.33}$$

In summary, for a given initial value $U_0 \in L^2(\Omega)$, the CSLDG numerical solution of Eq.(1.1) under compact-support boundary conditions is unconditionally stable, and we have

$$\|U_h^n - W_h^n\|_{L^2(\Omega)}^2 \le C \|U_0 - W_0\|_{L^2(\Omega)}^2, \quad \forall W_0 \in L^2(\Omega) \ (n = 1, 2, \ldots, N), \tag{3.34}$$

where

$$C = \max\{e^{M_A \Delta t/2} C_0, e^{M_A \cdot 2\Delta t/2} C_1 \cdot C_0, \ldots, e^{M_A \cdot N \Delta t/2} \prod_{i=0}^{N-1} C_i\} > 0 \tag{3.35}$$

depends only on $(T, \Delta t, \Omega, \mathbf{A})$ but independent of h.

Setting $W_0 \equiv 0$ yields the estimate (3.17). □

Remark 3.6. *Compared to* (3.17)*, equation* (3.34) *represents a more general form of numerical stability.*

Remark 3.7. *From Lemma 3.4, we know that the constants* C_k $(k = 0, 1, 2, \ldots, N-1)$ *appearing in the proof of Theorem 3.2 essentially reflect the scaling of the* L^2*-norm during the process of extending a* L^2*-function from the bounded domain* Ω *to another bounded domain* $\widetilde{\Omega}^{k+1,k}$ *via periodic extension or zero extension. Since* Ω *and* $\widetilde{\Omega}^{k+1,k}$ *evolve according to the characteristic equation* $\frac{\mathrm{dx}}{\mathrm{dt}} = \mathbf{A}(\mathbf{x}, t)$ *over the time interval* $[t_k, t_{k+1}]$*, the constants* C_k *depend on* $(\Omega, \mathbf{A}, t_k, t_{k+1})$ *but are independent of the mesh size* h*, because the norms involved in the inequalities controlled by* C_k *are defined on the entire spatial computational domain, namely* $\|\cdot\|_{L^2(\Omega)}$ *and* $\|\cdot\|_{L^2(\widetilde{\Omega}^{i+1,i})}$*, rather than on any individual grid cell* $\Omega_{\mathcal{K}}$ *or* $\widetilde{\Omega}^{i+1,i}_{\mathcal{K}}$ *— a point already clarified in Lemma 3.4. To ensure that Eq.*(3.34) *holds at all discrete time levels* $(n = 1, 2, \ldots, N)$*, we take*

$$\max\{e^{M_A \Delta t/2} C_0, e^{M_A \cdot 2\Delta t/2} C_1 \cdot C_0, \ldots, e^{M_A \cdot N \Delta t/2} \prod_{i=0}^{N-1} C_i\},$$

and this "maximization" operation causes the final control constant C *in Eq.*(3.34) *to also depend on the total time* T*, as the number of time steps* N *is determined by* T *and the time step size* Δt*. Under the premise of a uniform partition of* T*, once the time step* Δt *is introduced, the time points* (t_k, t_{k+1}) *are determined by* $(T, \Delta t)$*. Consequently,* C *depends on* $(T, \Delta t, \Omega, \mathbf{A})$ *but is independent of the spatial step size* h*.*

Theorem 3.3. *For a given initial value* $U_0 \in L^2(\Omega)$*, the CSLDG numerical solution sequence* $\{U_h^n\}(n = 1, 2, \ldots, N)$ *defined as Definition 2.1 is unique.*

Proof. Let U_h^n and W_h^n be two different CSLDG numerical solutions to equation (1.1) under the same initial and boundary conditions. That is, for all $\Omega_{\mathcal{K}} \in \mathcal{T}_h$, the following holds:

$$\int_{\Omega_{\mathcal{K}}} U_h^{n+1}|_{\Omega_{\mathcal{K}}} \cdot \Psi^{(\mathcal{K})} \, \mathrm{d}\mathbf{x} = \int_{\widetilde{\Omega}^{n+1,n}_{\mathcal{K}}} \widetilde{U}_h^n|_{\widetilde{\Omega}^{n+1,n}_{\mathcal{K}}} \cdot \psi^n_{\mathcal{K}}(\mathbf{x}; \Psi^{(\mathcal{K})}) \, \mathrm{d}\mathbf{x}, \ \forall \Psi^{(\mathcal{K})} \in H_0(\Omega_{\mathcal{K}}), \tag{3.36a}$$

$$\int_{\Omega_{\mathcal{K}}} W_h^{n+1}|_{\Omega_{\mathcal{K}}} \cdot \Psi^{(\mathcal{K})} \, \mathrm{d}\mathbf{x} = \int_{\widetilde{\Omega}^{n+1,n}_{\mathcal{K}}} \widetilde{W}_h^n|_{\widetilde{\Omega}^{n+1,n}_{\mathcal{K}}} \cdot \psi^n_{\mathcal{K}}(\mathbf{x}; \Psi^{(\mathcal{K})}) \, \mathrm{d}\mathbf{x}, \ \forall \Psi^{(\mathcal{K})} \in H_0(\Omega_{\mathcal{K}}). \tag{3.36b}$$

Subtracting (3.36b) from (3.36a), we obtain:

$$\int_{\Omega_{\mathcal{K}}} \left(U_h^{n+1}|_{\Omega_{\mathcal{K}}} - W_h^{n+1}|_{\Omega_{\mathcal{K}}}\right) \cdot \Psi^{(\mathcal{K})} \, \mathrm{d}\mathbf{x} = \int_{\widetilde{\Omega}^{n+1,n}_{\mathcal{K}}} \left(\widetilde{U}_h^n|_{\widetilde{\Omega}^{n+1,n}_{\mathcal{K}}} - \widetilde{W}_h^n|_{\widetilde{\Omega}^{n+1,n}_{\mathcal{K}}}\right) \cdot \psi^n_{\mathcal{K}}(\mathbf{x}; \Psi^{(\mathcal{K})}) \, \mathrm{d}\mathbf{x}, \ \forall \Psi^{(\mathcal{K})} \in H_0(\Omega_{\mathcal{K}}). \tag{3.37}$$

Now, choose

$$\Psi^{(\mathcal{K})} = U_h^{n+1}|_{\Omega_{\mathcal{K}}} - W_h^{n+1}|_{\Omega_{\mathcal{K}}}. \tag{3.38}$$

Since $U_h^{n+1}, W_h^{n+1} \in H_0(\Omega)$, it follows that $\Psi^{(\mathcal{K})} \in H_0(\Omega_{\mathcal{K}})$.

- For $n = 1$, following the proof process of Theorem 3.2, we still have

$$\|U_h^1|_{\Omega_\mathcal{K}} - W_h^1|_{\Omega_\mathcal{K}}\|_{L^2(\Omega_\mathcal{K})} \le e^{M_A \Delta t/2} \|\widetilde{U}_h^0|_{\widetilde{\Omega}_\mathcal{K}^{1,0}} - \widetilde{W}_h^0|_{\widetilde{\Omega}_\mathcal{K}^{1,0}}\|_{L^2(\widetilde{\Omega}_\mathcal{K}^{1,0})}, \tag{3.39}$$

The difference is that the uniqueness proof is carried out under the same initial condition, i.e., $U_0 \equiv W_0$. Therefore, $\Pi(U_0, \mathbb{D}\{\widetilde{\Omega}_\mathcal{K}^{1,0}\}) = \Pi(W_0, \mathbb{D}\{\widetilde{\Omega}_\mathcal{K}^{1,0}\})$, which implies $\widetilde{U}_h^0|_{\widetilde{\Omega}_\mathcal{K}^{1,0}} = \widetilde{W}_h^0|_{\widetilde{\Omega}_\mathcal{K}^{1,0}}$. Thus,

$$\|U_h^1|_{\Omega_\mathcal{K}} - W_h^1|_{\Omega_\mathcal{K}}\|_{L^2(\Omega_\mathcal{K})} = 0, \tag{3.40}$$

which means

$$U_h^1|_{\Omega_\mathcal{K}} = W_h^1|_{\Omega_\mathcal{K}} \quad \text{a.e. in } \Omega_\mathcal{K}, \quad \forall \Omega_\mathcal{K} \in \mathcal{T}_h. \tag{3.41}$$

Therefore,

$$U_h^1 = W_h^1 \quad \text{a.e. in } \Omega. \tag{3.42}$$

- Finally, using mathematical induction again, we obtain

$$U_h^n = W_h^n \quad \text{a.e. in } \Omega \quad (n = 1, 2, \ldots, N). \tag{3.43}$$

In conclusion, for a given initial condition U_0, the CSLDG numerical solution U_h^n $(n = 1, 2, \ldots, N)$ to equation (1.1) under compact-support boundary conditions is unique in the sense of L^2-norm. □

4. A Novel Implementation of Dimension Splitting in CSLDG Framework

4.1. **Dimension Splitting.**

In this section, we consider two-dimensional problems. Let the two-dimensional differential operator be $\mathcal{L}_{xy}$, and the two-dimensional control equation is given by

$$U_t = \mathcal{L}_{xy} U.$$

For the two-dimensional linear scalar transport equation, we have $\mathcal{L}_{xy} = a(x, y, t)\partial_x + b(x, y, t)\partial_y$.

The variable-separation-based dimensional splitting implementation proposed in this paper is applicable to splitting schemes of arbitrary order. The numerical examples in Section 5 include both the 2nd-order Strang splitting[13, 20] and the 4th-order Strang splitting(also known as Ruth splitting)[21, 22, 23]. Therefore, we first provide the detailed steps for these two splitting schemes here:

- The 2nd-order Strang splitting scheme for evolving from t^n to t^{n+1} consists of three sub-steps:

$$\begin{aligned}
t^n: &\quad U^n;\\
\text{stage 1}: &\quad \partial_t U^{(x)} = \mathcal{L}_x U^{(x)} \quad , \quad U^{(x)}(t^n) = U^n \quad , \quad t^n \to t^{n+1/2};\\
\text{stage 2}: &\quad \partial_t U^{(y)} = \mathcal{L}_y U^{(y)} \quad , \quad U^{(y)}(t^n) = U^{(x)}(t^{n+1/2}) \quad , \quad t^n \to t^{n+1};\\
\text{stage 3}: &\quad \partial_t U^{(x)} = \mathcal{L}_x U^{(x)} \quad , \quad U^{(x)}(t^{n+1/2}) = U^{(y)}(t^{n+1}) \quad , \quad t^{n+1/2} \to t^{n+1};\\
t^{n+1}: &\quad U^{n+1} = U^{(x)}(t^{n+1}).
\end{aligned}$$

- A 4th-order Strang splitting scheme is considered for evolving the solution from t^n to t^{n+1}, divided into 7 substeps as follows:
  stage 1: evolve $u_t + (au)_x = 0$ for $c_1\Delta t^n$;
  stage 2: evolve $u_t + (bu)_y = 0$ for $d_1\Delta t^n$;
  stage 3: evolve $u_t + (au)_x = 0$ for $c_2\Delta t^n$;
  stage 4: evolve $u_t + (bu)_y = 0$ for $d_2\Delta t^n$;
  stage 5: evolve $u_t + (au)_x = 0$ for $c_3\Delta t^n$;
  stage 6: evolve $u_t + (bu)_y = 0$ for $d_3\Delta t^n$;
  stage 7: evolve $u_t + (au)_x = 0$ for $c_4\Delta t^n$,
  where the coefficients are given by:

$$d_1 = d_3 = \frac{1}{2-2^{1/3}} \approx 1.3512, \qquad d_2 = -\frac{2^{1/3}}{2-2^{1/3}} \approx -1.7024,$$
$$c_1 = c_4 = \frac{d_1}{2} \approx 0.6756, \qquad c_2 = c_3 = \frac{d_1+d_2}{2} \approx -0.1756.$$

Remark 4.1 (General Pattern of Strang Dimensional Splitting Schemes)**.** *Consider evolving from t^n to t^{n+1} with a time step size $\Delta t^n = t^{n+1} - t^n$. If a $p+q$-step "x-y-x" type dimensional splitting scheme is used, let the set of substep sizes for the x-direction be $\{c_i\Delta t^n\}_{i=1}^p$ and for the y-direction be $\{d_j\Delta t^n\}_{j=1}^q$. Then, the following conditions must be satisfied:*

$$p = q+1, \quad \sum_{i=1}^{p} c_i = 1, \quad \sum_{j=1}^{q} d_j = 1.$$

x-direction:

$$\text{stage } 2k-1: \quad \text{evolve} \quad t^n + \sum_{i=1}^{k-1} c_i\Delta t^n \quad \text{into} \quad t^n + \sum_{i=1}^{k-1} c_i\Delta t^n + c_k\Delta t^n,$$

where $k = 1, 2, \ldots, p$;

y-direction:

$$\text{stage } 2k: \quad \text{evolve} \quad t^n + \sum_{j=1}^{k-1} d_j\Delta t^n \quad \text{into} \quad t^n + \sum_{j=1}^{k-1} d_j\Delta t^n + d_k\Delta t^n,$$

where $k = 1, 2, \ldots, q$.

4.2. **A Separated Variable-Type Implementation for Dimension Splitting.**

The two-dimensional linear scalar transport equation is given by:

$$\partial_t U(x,y,t) + \partial_x(a(x,y,t)U(x,y,t)) + \partial_y(b(x,y,t)U(x,y,t)) = 0 \quad \text{in } D \subset \mathbb{R}^2. \tag{4.1}$$

The 2D rectangular computational domain is defined as:

$$D = I^x \times I^y;$$

The partitions of I^x and I^y are given by:

$$I^x = I_1^x \cup I_2^x \cup I_3^x \cup \cdots \cup I_{N_x}^x,$$
$$I^y = I_1^y \cup I_2^y \cup I_3^y \cup \cdots \cup I_{N_y}^y;$$

Accordingly, the partition of D is:

$$\begin{aligned} D =& E_1^1 \cup E_2^1 \cup E_3^1 \cup \cdots \cup E_{N_y}^1 \cup E_1^2 \cup E_2^2 \cup E_3^2 \cup \cdots \cup E_{N_y}^2 \cup \\ & E_1^3 \cup E_2^3 \cup E_3^3 \cup \cdots \cup E_{N_y}^3 \cup \cdots \cup E_1^{N_x} \cup E_2^{N_x} \cup E_3^{N_x} \cup \cdots \cup E_{N_y}^{N_x}. \end{aligned}$$

Consider the element (e) satisfying $(e) = E_s^r = I_r^x \times I_s^y$. The DG approximation solution on element (e) is:

$$U^{(e)}(x,y,t) = \sum_{i=0}^{K_x} \alpha_i^{(r)}(y,t)\phi_i^{(r)}(x), \tag{4.2}$$

where

$$\alpha_i^{(r)}(y,t) = \sum_{j=0}^{K_y} \beta_{i,j}^{(r,s)}(t)\varphi_j^{(s)}(y), \tag{4.3}$$

Thus, we have

$$U^{(e)}(x,y,t) = \sum_{i=0}^{K_x}\sum_{j=0}^{K_y} \beta_{i,j}^{(r,s)}(t)\varphi_j^{(s)}(y)\phi_i^{(r)}(x). \tag{4.4}$$

In the proposed variable-separation-based dimensional splitting scheme, the set $\left\{\beta_{i,j}^{(r,s)}\right\}$ represents the target coefficients to be solved at each stage of the dimensional splitting. This implies that the intermediate and final results of our dimensional splitting remain as two-dimensional polynomials, which is different from the schemes in [1, 4]. In those schemes, the direct output is a family of one-dimensional polynomials at certain numerical integration points. Therefore, interpolation is required to obtain the intermediate initial conditions for the other direction during dimension switching, and the final results (one-dimensional polynomials) need to be post-processed through interpolation to obtain the two-dimensional polynomial or the approximate value of the field function at non-integration points. In contrast, our approach evolves two-dimensional polynomials directly. Therefore, no interpolation is needed during dimension switching; the intermediate initial conditions for the other dimension can be obtained simply by fixing the corresponding coordinate. For the final results, the approximate value of the field function at any point within the computational

domain can be obtained by directly substituting the coordinates of that point. For convenience in notation, the element index (e) and the indices (r) and (s) in the basis functions and modal coefficients are omitted in the subsequent algorithm construction process.

Consider evolving from t^n to t^{n+1} using a $p+q$-step "x-y-x" type dimensional splitting scheme. Let the set of sub-time steps in the x-direction be $\{t_c^x\}_{c=1}^p$, and the set of sub-time steps in the y-direction be $\{t_d^y\}_{d=1}^q$. The alternating evolution route is as follows:

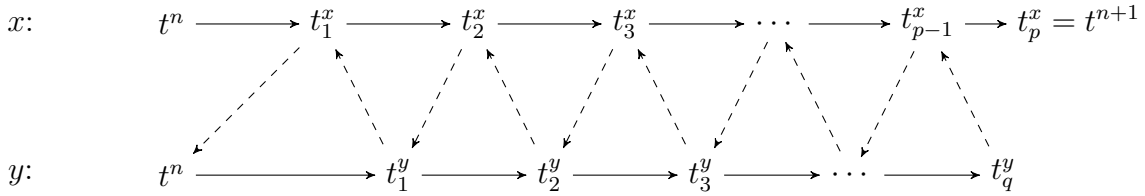

Here, the symbol "$\rightarrow$" denotes solving the governing equations (in this context, solving the integral invariant model), while "$\dashrightarrow$" denotes assignment, where the intermediate result from one direction serves as the initial condition for the evolution in the other direction. Therefore, the evolution process strictly follows the sequence of "solid line $\rightarrow$ dashed line $\dashrightarrow$ solid line $\rightarrow$".

Fix $y = [Gg]_s^y \in I_s^y$, then the transport equation in the x-direction is

$$\partial_t U + \partial_x(a(x, [Gg]_s^y, t)U(x, [Gg]_s^y, t)) = 0. \tag{4.5}$$

The integral invariant in the x-direction is

$$\int_{I_r^x} U(x, [Gg]_s^y, t_{c+1}^x)\Psi^x(x)dx = \int_{I_r^{x,\star}} U(x, [Gg]_s^y, t_d^x)\psi^x(x, t_c^x)dx; \tag{4.6}$$

fix $x = [Gg]_r^x \in I_r^x$, the transport equation in the y-direction is

$$\partial_t U + \partial_y(b([Gg]_r^x, y, t)U([Gg]_r^x, y, t)) = 0, \tag{4.7}$$

and the integral invariant in the y-direction is

$$\int_{I_s^y} U([Gg]_r^x, y, t_{d+1}^y)\Psi^y(y)dy = \int_{I_s^{y,\star}} U([Gg]_r^x, y, t_d^y)\psi^y(y, t_d^y)dy. \tag{4.8}$$

- **Solving the integral invariant in the x-direction after dimensional splitting**

Taking $\Psi^x = \phi_k(x),\ k = 0, 1, 2, \cdots, K_x$, we have

$$\underbrace{\int_{I_r^x} U(x, [Gg]_s^y, t_{c+1}^x)\phi_k(x)dx}_{LHS_r^x(k,[Gg]_s^y;d+1)} = \underbrace{\int_{I_r^{x,\star}} U(x, [Gg]_s^y, t_{ds}^x)\psi^x(x, t_c^x; \phi_k)dx}_{RHS_r^x(k,[Gg]_s^y;d)} \tag{4.9}$$

Substituting Eq.(4.4) into the calculation, we obtain

$$\begin{aligned} LHS_r^x(k, [Gg]_s^y; c+1) &= \int_{I_r^x} \left[\sum_{i=0}^{K_x}\sum_{j=0}^{K_y} \beta_{i,j}(t_{c+1}^x)\varphi_j([Gg]_s^y)\phi_i(x)\right] \cdot \phi_k(x)dx \\ &= \sum_{j=0}^{K_y} \varphi_j([Gg]_s^y)\beta_{k,j}(t_{c+1}^x), \end{aligned} \tag{4.10}$$

whose matrix form is

$$LHS_r^x(k,[Gg]_s^y;c+1)=\left[\beta_{k,0}^{c+1},\beta_{k,1}^{c+1},\beta_{k,2}^{c+1},\cdots,\beta_{k,K_y}^{c+1}\right]\begin{bmatrix}\varphi_0([Gg]_s^y)\\ \varphi_1([Gg]_s^y)\\ \varphi_2([Gg]_s^y)\\ \vdots\\ \varphi_{K_y}([Gg]_s^y)\end{bmatrix}. \tag{4.11}$$

Letting $[Gg]_s^y$ traverse $\left\{[G0]_s^y,[G1]_s^y,[G2]_s^y,\cdots,[GK_y]_s^y\right\}\subset I_s^y$, we obtain

$$\begin{aligned}&LHS_r^x(k,:;c+1)\\&=\left[LHS_r^x(k,[G0]_s^y;c+1),\ LHS_r^x(k,[G1]_s^y;c+1),\ LHS_r^x(k,[G2]_s^y;c+1),\ \cdots,\ LHS_r^x(k,[GK_y]_s^y;c+1)\right]\\&=\left[\beta_{k,0}^{c+1},\beta_{k,1}^{c+1},\beta_{k,2}^{c+1},\cdots,\beta_{k,K_y}^{c+1}\right]\begin{bmatrix}\varphi_0([G0]_s^y)&\varphi_0([G1]_s^y)&\varphi_0([G2]_s^y)&\cdots&\varphi_0([GK_y]_s^y)\\ \varphi_1([G0]_s^y)&\varphi_1([G1]_s^y)&\varphi_1([G2]_s^y)&\cdots&\varphi_1([GK_y]_s^y)\\ \varphi_2([G0]_s^y)&\varphi_2([G1]_s^y)&\varphi_2([G2]_s^y)&\cdots&\varphi_2([GK_y]_s^y)\\ \vdots&\vdots&\vdots&\vdots&\vdots\\ \varphi_{K_y}([G0]_s^y)&\varphi_{K_y}([G1]_s^y)&\varphi_{K_y}([G2]_s^y)&\cdots&\varphi_{K_y}([GK_y]_s^y)\end{bmatrix}\end{aligned} \tag{4.12}$$

and let Ψ^x traverse $\{\phi_0(x),\phi_1(x),\phi_2(x),\cdots,\phi_{K_x}(x)\}$, yielding

$$\begin{aligned}LHS_r^x(c+1)&=\left[LHS_r^x(0,:;c+1)^{\mathrm{T}},LHS_r^x(1,:;c+1),LHS_r^x(2,:;c+1)^{\mathrm{T}},\cdots,LHS_r^x(K_x,:;c+1)^{\mathrm{T}}\right]^{\mathrm{T}}\\&=\begin{bmatrix}\beta_{0,0}^{c+1}&\beta_{0,1}^{c+1}&\beta_{0,2}^{c+1}&\cdots&\beta_{0,K_y}^{c+1}\\ \beta_{1,0}^{c+1}&\beta_{1,1}^{c+1}&\beta_{1,2}^{c+1}&\cdots&\beta_{1,K_y}^{c+1}\\ \beta_{2,0}^{c+1}&\beta_{2,1}^{c+1}&\beta_{2,2}^{c+1}&\cdots&\beta_{2,K_y}^{c+1}\\ \vdots&\vdots&\vdots&\vdots&\vdots\\ \beta_{K_x,0}^{c+1}&\beta_{K_x,1}^{c+1}&\beta_{K_x,2}^{c+1}&\cdots&\beta_{K_x,K_y}^{c+1}\end{bmatrix}_{K_x+1\times K_y+1}\times\\&\quad\begin{bmatrix}\varphi_0([G0]_s^y)&\varphi_0([G1]_s^y)&\varphi_0([G2]_s^y)&\cdots&\varphi_0([GK_y]_s^y)\\ \varphi_1([G0]_s^y)&\varphi_1([G1]_s^y)&\varphi_1([G2]_s^y)&\cdots&\varphi_1([GK_y]_s^y)\\ \varphi_2([G0]_s^y)&\varphi_2([G1]_s^y)&\varphi_2([G2]_s^y)&\cdots&\varphi_2([GK_y]_s^y)\\ \vdots&\vdots&\vdots&\vdots&\vdots\\ \varphi_{K_y}([G0]_s^y)&\varphi_{K_y}([G1]_s^y)&\varphi_{K_y}([G2]_s^y)&\cdots&\varphi_{K_y}([GK_y]_s^y)\end{bmatrix}_{K_y+1\times K_y+1}\\&=[\beta]_{(r,s)}^{x,c+1}[\Phi]_s^y.\end{aligned} \tag{4.13}$$

For notational convenience, let

$$J_{k,g}^{xr}(c):=\int_{I_r^{x,\star}}U(x,(Gg)_s^y,t_c^x)\psi^x(x,t_c^x;\phi_k)dx,\ g=0,1,2,\cdots,K_y, \tag{4.14}$$

thus $RHS_r^x(k,[Gg]_s^y;c)=J_{k,g}^{xr}(c)$.
Let $[Gg]_s^y$ iterate over $\left\{[G0]_s^y,[G1]_s^y,[G2]_s^y,\cdots,[GK_y]_s^y\right\}\subset I_r^x$, yielding

$$RHS_r^x(k,:;c)=\begin{bmatrix}J_{k,0}^{xr}(c)&J_{k,1}^{xr}(c)&J_{k,2}^{xr}(c)&\cdots&J_{k,K_y}^{xr}(c)\end{bmatrix}, \tag{4.15}$$

and let Ψ^x iterate over $\{\phi_0(x), \phi_1(x), \phi_2(x), \cdots, \phi_{K_x}(x)\}$, resulting in

$$RHS_r^x(c) = \left[RHS_r^x(0,:;c)^{\mathrm{T}}, RHS_r^x(1,:;c)^{\mathrm{T}}, RHS_r^x(2,:;c)^{\mathrm{T}}, \cdots, RHS_r^x(K_x,:;c)^{\mathrm{T}}\right]^{\mathrm{T}}$$
$$= \begin{bmatrix} J_{0,0}^{xr}(c) & J_{0,1}^{xr}(c) & J_{0,2}^{xr}(c) & \cdots & J_{0,K_y}^{xr}(c) \\ J_{1,0}^{xr}(c) & J_{1,1}^{xr}(c) & J_{1,2}^{xr}(c) & \cdots & J_{1,K_y}^{xr}(c) \\ J_{2,0}^{xr}(c) & J_{2,1}^{xr}(c) & J_{2,2}^{xr}(c) & \cdots & J_{2,K_y}^{xr}(c) \\ \vdots & \vdots & \vdots & \vdots & \vdots \\ J_{K_x,0}^{xr}(c) & J_{K_x,1}^{xr}(c) & J_{K_x,2}^{xr}(c) & \cdots & J_{K_x,K_y}^{xr}(c) \end{bmatrix}_{K_x+1\times K_y+1}. \tag{4.16}$$

Remark 4.2. *$U(x,(Gg)_s^y,t_c^x) = \sum_{i=0}^{K_x}\sum_{j=0}^{K_y}\beta_{i,j}(t_c^x)\varphi_j((Gg)_s^y)\phi_i(x)$ degenerates into a univariate function of x. Note that $U(x,(Gg)_s^y,t_c^x)$ contains not only $\phi(x)$ but also $\varphi(y)$. If a 2D program is used to compute its function value, then $(x^q,(Gg)_s^y)$ should be substituted, where x^q is a 1D-Gauss/Gauss-Lobatto-Legendre point.*

Thus, we have

$$LHS_r^x(c+1) = RHS_r^x(c), \tag{4.17a}$$
$$[\beta]_{(r,s)}^{x,c+1}[\Phi]_s^y = RHS_r^x(c), \tag{4.17b}$$
$$[\beta]_{(r,s)}^{x,c+1} = RHS_r^x(c)\left([\Phi]_s^y\right)^{-1}. \tag{4.17c}$$

• **Solving the integral invariant in the y-direction after dimensional splitting**

The computational procedure follows analogously to the x-direction. Since readers can readily derive it by following the procedure outlined above, the details are not repeated here for brevity.

5. Numerical Results

5.1. Accuracy Tests for 2D-CSLDG based on Separated Variable's Splitting.

Example 5.1. *Linear transport problem with constant advection coefficients.*
Control Eqs:

$$U_t + U_x + U_y = 0;$$

Computational Domain:

$$\Omega\times[0,T_{end}] = \{[-\pi,\pi]\times[-\pi,\pi]\}\times[0,\pi];$$

BCs: periodic boundary conditions;

- *ICs:*

$$U(x,y,0) = \cos(x-y);$$

True solution:

$$U(x,y,t) = \cos(x-y),\ \forall t\in[0,+\infty).$$

Based on separated variable's splitting in CSLDG-A1 framework, L^∞, L^2, L^1 numerical errors and convergence orders for U with Q^2- and Q^3- polynomial approximations are shown in Table 1.

TABLE 1. CSLDG-A1 for constant advection coefficients.

CSLDG-A1	**separated variable's splitting**					
Mesh	L^2 *error*	*Order*	L^1 *error*	*Order*	L^∞ *error*	*Order*
Q^2 CFL = 10.5 2^{nd}-Strang						
16^2	*8.65E-4*	——	*4.17E-3*	——	*4.05E-4*	——
32^2	*1.03E-4*	*3.07*	*4.87E-4*	*3.10*	*4.36E-5*	*3.22*
64^2	*1.38E-5*	*2.90*	*6.26E-5*	*2.96*	*5.93E-6*	*2.88*
128^2	*1.05E-6*	*3.71*	*4.87E-6*	*3.68*	*4.83E-7*	*3.62*
256^2	*1.30E-7*	*3.02*	*6.10E-7*	*3.00*	*6.04E-8*	*3.00*
512^2	*1.63E-8*	*3.00*	*7.62E-8*	*3.00*	*7.55E-9*	*3.00*
Q^3 CFL = 5 4^{th}-Strang						
10^2	*1.52E-3*	——	*7.33E-3*	——	*6.52E-4*	——
20^2	*1.39E-4*	*3.45*	*6.80E-4*	*3.43*	*5.61E-5*	*3.54*
40^2	*9.49E-6*	*3.87*	*4.59E-5*	*3.89*	*3.38E-6*	*4.05*
80^2	*3.83E-7*	*4.63*	*1.86E-6*	*4.63*	*1.45E-7*	*4.54*
160^2	*5.55E-9*	*6.11*	*2.87E-8*	*6.01*	*1.96E-9*	*6.22*
320^2	*1.77E-10*	*4.97*	*8.29E-10*	*5.12*	*7.65E-11*	*4.68*

- *ICs:*

$$U(x, y, 0) = \sin(x + y);$$

True solution:

$$U(x, y, t) = \sin(x + y - 2t).$$

Based on separated variable's splitting in CSLDG-A2 framework, L^∞, L^2, L^1 numerical errors and convergence orders for U with Q^2- and Q^3-polynomial approximations are shown in Table 2.

Example 5.2. *Rigid body rotation.*
Control Eqs:

$$U_t - (4\sqrt{2}yU)_x + (2\sqrt{2}xU)_y = 0;$$

Computational Domain:

$$\Omega \times [0, T_{end}] = \{[-1.5, 1.5] \times [-0.75, 0.75]\} \times [0, \pi/2];$$

ICs:

$$U(x, y, 0) = \exp\left(-x^2 - 5y^2\right);$$

BCs: periodic bouondary conditions;
True Solution:

$$U(x, y, T_{end}) = U_0(x, y), \ T_{end} = k \cdot \frac{\pi}{2}, \ k \in \mathbb{Z}^+.$$

TABLE 2. CSLDG-A2 for constant advection coefficients.

CSLDG-A2	**separated variable's splitting**					
Mesh	L^2 *error*	*Order*	L^1 *error*	*Order*	L^∞ *error*	*Order*
Q² CFL = 5.5 2nd-Strang						
8^2	*6.68E-3*	——	*3.14E-2*	——	*2.52E-3*	——
16^2	*7.84E-4*	*3.09*	*3.65E-3*	*3.10*	*3.26E-4*	*2.95*
32^2	*1.10E-4*	*2.83*	*5.40E-4*	*2.76*	*5.31E-5*	*2.62*
64^2	*1.33E-5*	*3.05*	*6.19E-5*	*3.13*	*6.09E-6*	*3.12*
128^2	*1.04E-6*	*3.67*	*4.94E-6*	*3.65*	*4.22E-7*	*3.85*
256^2	*2.17E-7*	*2.26*	*1.05E-6*	*2.23*	*8.88E-8*	*2.25*
512^2	*2.56E-8*	*3.08*	*1.24E-7*	*3.08*	*1.23E-8*	*2.85*
Q³ CFL = 2.5 2nd-Strang						
8^2	*3.51E-3*	——	*1.66E-2*	——	*1.54E-3*	——
16^2	*3.72E-4*	*3.24*	*1.82E-3*	*3.19*	*1.64E-4*	*3.23*
32^2	*3.45E-5*	*3.43*	*1.64E-4*	*3.47*	*1.51E-5*	*3.45*
64^2	*2.34E-6*	*3.88*	*1.16E-5*	*3.82*	*8.92E-7*	*4.08*
128^2	*1.11E-7*	*4.41*	*6.21E-7*	*4.23*	*2.86E-8*	*4.96*
256^2	*1.25E-9*	*6.46*	*6.29E-9*	*6.63*	*3.99E-10*	*6.16*

- *Based on separated variable's splitting in CSLDG-A1 framework, L^∞, L^2, L^1 numerical errors and convergence orders for U with Q^2- and Q^3- polynomial approximations are shown in Table 3.*

TABLE 3. CSLDG-A1 for RigidBody.

CSLDG-A1	**separated variable's splitting**					
Mesh	L^2 *error*	*Order*	L^1 *error*	*Order*	L^∞ *error*	*Order*
Q² CFL = 20 2nd-Strang						
20^2	*1.41E-0*	——	*5.59E-0*	——	*9.82E-1*	——
40^2	*4.78E-1*	*1.56*	*1.52E-0*	*1.88*	*2.82E-1*	*1.80*
80^2	*1.82E-2*	*4.72*	*5.83E-2*	*4.71*	*1.07E-2*	*4.72*
160^2	*1.01E-3*	*4.16*	*3.35E-3*	*4.12*	*5.95E-4*	*4.16*
320^2	*7.41E-5*	*3.77*	*2.73E-4*	*3.62*	*6.09E-5*	*3.29*

- *Based on separated variable's splitting in CSLDG-A2 framework, L^∞, L^2, L^1 numerical errors and convergence orders for U with Q^2- and Q^3- polynomial approximations are shown in Table 4.*

Example 5.3. *Swirling deformation flow.*
Control Eqs: $U_t - \left(\cos^2\left(\frac{x}{2}\right)\sin(y)g(t)U\right)_x + \left(\sin(x)\cos^2\left(\frac{y}{2}\right)g(t)U\right)_y = 0,$
where $g(t) = 2\pi\cos(\pi t/T), \quad T = 1.5;$
Computational Domain: $\Omega \times [0, T_{end}] = \{[-\pi, \pi] \times [-\pi, \pi]\} \times [0, 1.5];$
ICs:

$$U(x, y, 0) = \begin{cases} r_0^b \cos\left(\frac{r^b(\mathbf{x})\pi}{2r_0^b}\right)^6, & \text{if } r^b(\mathbf{x}) < r_0^b \\ 0, & \text{otherwise} \end{cases}$$

TABLE 4. CSLDG-A2 for RigidBody.

CSLDG-A2	**separated variable's splitting**					
Mesh	L^2 *error*	*Order*	L^1 *error*	*Order*	L^∞ *error*	*Order*
Q² CFL = 10.5 2nd-Strang						
20^2	*3.26E-1*	——	*1.05E-0*	——	*1.92E-1*	——
40^2	*1.81E-2*	*4.17*	*5.82E-2*	*4.17*	*1.07E-2*	*4.16*
80^2	*1.31E-3*	*3.79*	*4.31E-3*	*3.76*	*7.75E-4*	*3.78*
160^2	*4.36E-4*	*1.59*	*1.46E-3*	*1.56*	*2.56E-4*	*1.60*
320^2	*3.12E-5*	*3.80*	*8.30E-5*	*4.14*	*5.46E-5*	*2.23*
Q² CFL = 2.5 2nd-Strang						
10^2	*2.09E-2*	——	*6.90E-2*	——	*1.62E-2*	——
20^2	*1.45E-3*	*3.85*	*4.57E-3*	*3.92*	*1.72E-3*	*3.23*
40^2	*1.22E-4*	*3.57*	*4.22E-4*	*3.44*	*1.46E-4*	*3.57*
80^2	*1.80E-5*	*2.77*	*6.41E-5*	*2.72*	*1.60E-5*	*3.18*

where $r_0^b = 0.3\pi,\ r^b(\mathbf{x}) = \sqrt{\left(x - x_0^b\right)^2 + \left(y - y_0^b\right)^2},\ \left(x_0^b, y_0^b\right) = (0.3\pi, 0)$*;*
BCs: periodic boundary conditions;
True Solution: along the direction of the flow, the initial function becomes largely deformed at $t = T/2$*, then goes back to its initial shape at* $t = T$ *as the flow reverses, i.e.,*

$$U(x, y, T) = U_0(x, y).$$

- *Based on separated variable's splitting in CSLDG-A1 framework,* L^∞*,* L^2*,* L^1 *numerical errors and convergence orders for* U *with* Q^2*- and* Q^3*- polynomial approximations are shown in Table 5.*

TABLE 5. CSLDG-A1 for Swirling.

CSLDG-A1	**separated variable's splitting**					
Mesh	L^2 *error*	*Order*	L^1 *error*	*Order*	L^∞ *error*	*Order*
Q² CFL = 2.5 4th-Strang						
20^2	*2.25E-1*	——	*2.81E-1*	——	*5.79E-1*	——
40^2	*4.01E-2*	*2.49*	*3.37E-2*	*3.06*	*1.04E-1*	*2.47*
80^2	*7.51E-4*	*5.74*	*5.87E-4*	*5.84*	*3.29E-3*	*4.99*
160^2	*3.39E-5*	*4.47*	*2.99E-5*	*4.30*	*1.96E-4*	*4.06*
320^2	*1.61E-6*	*4.39*	*1.52E-6*	*4.30*	*9.41E-6*	*4.38*
640^2	*1.77E-7*	*3.19*	*1.59E-7*	*3.26*	*8.19E-7*	*3.52*
Q³ CFL = 2.5 4th-Strang						
20^2	*3.01E-1*	——	*3.38E-1*	——	*8.27E-1*	——
40^2	*4.02E-2*	*2.90*	*3.33E-2*	*3.34*	*1.11E-1*	*2.90*
80^2	*5.10E-4*	*6.30*	*4.20E-4*	*6.31*	*2.13E-3*	*5.70*
160^2	*2.72E-5*	*4.23*	*2.34E-5*	*4.17*	*9.17E-5*	*4.54*
320^2	*3.41E-7*	*6.32*	*2.43E-7*	*6.59*	*2.57E-6*	*5.16*
640^2	*1.76E-8*	*4.28*	*1.31E-8*	*4.22*	*9.57E-8*	*4.75*

- *Based on separated variable's splitting in CSLDG-A2 framework,* L^∞*,* L^2*,* L^1 *numerical errors and convergence orders for* U *with* Q^2*- and* Q^3*- polynomial approximations are shown in Table 6.*

TABLE 6. CSLDG-A2 for Swirling.

CSLDG-A2	**separated variable's splitting**					
Mesh	L^2 *error*	*Order*	L^1 *error*	*Order*	L^∞ *error*	*Order*
Q^2 CFL = 2.5 4$^{\text{th}}$-Strang						
20^2	*1.67E-1*	——	*2.23E-1*	——	*3.72E-1*	——
40^2	*4.78E-2*	*1.81*	*4.02E-2*	*2.47*	*1.25E-1*	*1.58*
80^2	*8.48E-4*	*5.82*	*6.91E-4*	*5.86*	*3.13E-3*	*5.31*
160^2	*6.41E-5*	*3.73*	*5.11E-5*	*3.76*	*3.39E-4*	*3.21*
320^2	*5.21E-6*	*3.62*	*3.93E-6*	*3.70*	*3.11E-5*	*3.44*
Q^3 CFL = 2.5 4$^{\text{th}}$-Strang						
20^2	*2.38E-1*	——	*2.65E-1*	——	*5.51E-1*	——
40^2	*4.83E-2*	*2.30*	*4.00E-2*	*2.73*	*1.28E-1*	*2.11*
80^2	*7.20E-4*	*6.07*	*5.99E-4*	*6.06*	*1.73E-3*	*6.21*
160^2	*3.37E-5*	*4.41*	*2.87E-5*	*4.38*	*8.57E-5*	*4.34*
320^2	*3.75E-7*	*6.49*	*3.20E-7*	*6.49*	*1.62E-6*	*5.72*

5.2. **Comparison of Separated Variable's Splitting and Interpolation-based Splitting.**

Building on Examples 5.1 and 5.1 presented earlier, this subsection compares the numerical accuracy and computational efficiency of the proposed separated-variable dimensional-splitting implementation with the classical interpolation-based dimensional-splitting approach. **For brevity, our splitting scheme will be referred to as SVS, while the classical interpolation-based splitting approach will be denoted by IBS.**

• Linear transport problem with constant advection coefficients and $U(x, y, 0) = \cos(x - y)$ from Example 5.1.

The numerical errors and CPU times are summarized in the following Table 7 and Table 8, respectively.

TABLE 7. Numerical errors for constant advection coefficients with $U_0 = \cos(x - y)$: SVS vs IBS

CSLDG-A1	**separated variable's splitting**(SVS)						**Interpolation-based Splitting**(IBS)					
Mesh	L^2error	Order	L^1error	Order	L^∞error	Order	L^2error	Order	L^1error	Order	L^∞error	Order
Q^2 CFL = 10.5 2$^{\text{nd}}$-Strang												
16^2	8.65E-4	——	4.17E-3	——	4.05E-4	——	8.66E-4	——	4.17E-3	——	4.06E-4	——
32^2	1.03E-4	3.07	4.87E-4	3.10	4.36E-5	3.22	1.03E-4	3.07	4.87E-4	3.10	4.36E-5	3.23
64^2	1.38E-5	2.90	6.26E-5	2.96	5.93E-6	2.88	1.38E-5	2.90	6.26E-5	2.96	5.93E-6	2.88
128^2	1.05E-6	3.71	4.87E-6	3.68	4.83E-7	3.62	1.05E-6	3.71	4.87E-6	3.68	4.83E-7	3.62

TABLE 8. CPU time for constant advection coefficients with $U_0 = \cos(x - y)$: SVS vs IBS

CSLDG-A1 Q^2 CFL = 10.5 2$^{\text{nd}}$-Strang	CPU Time / s			
Mesh	16×16	32×32	64×64	128×128
separated variable's splitting(SVS)	5.8248	46.3964	334.9204	1712.0765
Interpolation-based Splitting(IBS)	3.9420	48.3791	785.0787	17761.7497

• Swirling deformation flow. from Example 5.3.

The numerical errors and CPU times are summarized in the following Table 9 and Table 10, respectively.

TABLE 9. Numerical errors for swirling deformation flow: SVS vs IBS

CSLDG-A2	**separated variable's splitting**(SVS)						**Interpolation-based Splitting**(IBS)					
Mesh	L^2error	Order	L^1error	Order	L^∞error	Order	L^2error	Order	L^1error	Order	L^∞error	Order
Q^3 CFL = 2.5 4^{th}-Strang												
20^2	2.38E-1	——	2.65E-1	——	5.51E-1	——	2.41E-1	——	2.49E-1	——	5.92E-1	——
40^2	4.83E-2	2.30	4.00E-2	2.73	1.28E-1	2.11	4.83E-2	2.32	4.00E-2	2.64	1.27E-1	2.22
80^2	7.20E-4	6.07	5.99E-4	6.06	1.73E-3	6.21	7.19E-4	6.07	5.98E-4	6.06	1.74E-3	6.20

TABLE 10. CPU time for swirling deformation flow: SVS vs IBS

CSLDG-A2 Q^3 CFL = 2.5 4^{th}-Strang	CPU Time / s		
Mesh	20×20	40×40	80×80
separated variable's splitting(SVS)	109.3606	884.7820	7012.2404
Interpolation-based Splitting(IBS)	333.7401	8730.8071	212645.9466

As shown in the tables above, the two dimensional splitting implementation schemes show **no significant difference in accuracy.** However, **the CPU time required for the separated variable-type dimensional splitting is significantly less than that of the interpolation-type dimensional splitting.** Moreover, **as the grid is continuously refined, the difference in computational efficiency between the two methods becomes more pronounced,** indicating that **the separated variable's splitting is more suitable for large-scale meshes.**

The higher computational efficiency of our scheme can be attributed to the following key aspects:

- **Explicit Matrix Construction:** Although the separated-variable dimensional splitting implementation involves a large number of matrices, all matrices except RHS_r^x are explicitly constructed during the algorithm derivation phase. Consequently, during actual code execution, only simple assignment operations are required, avoiding complex inter-matrix algebraic operations.
- **Inherent Numerical Integration:** The numerical integration associated with RHS_r^x is inherent to the CSLDG framework and unavoidable. It is crucial to note that traditional interpolation-based dimensional splitting schemes require numerical integration of identical complexity.
- **Additional Computational Overhead in Traditional Schemes:** However, each substep in traditional interpolation-based splitting schemes involves constructing an interpolation polynomial, which necessitates solving a linear system $\mathbb{A}\mathbf{x} = \mathbf{b}$. Generally speaking, the coefficient matrix $\mathbb{A}$ of the above normal equations derived from interpolation or fitting procedures is dense. When dealing with large-scale grid systems, this density can significantly degrade computational efficiency.
- **Potential Projection Overhead:** Furthermore, if the basis functions used for interpolation/fitting differ from the CSLDG basis functions, interpolation-based splitting

scheme requires an additional L^2-projection onto the basis function space, further increasing computational burden.

Therefore, the overall computational cost of interpolation-based dimensional splitting schemes substantially exceeds that of our separated-variable approach.

6. Conclusion

This paper demonstrates the existence of the numerical solution for the CSLDG method based on the Riesz representation theorem and analyzes the numerical stability of this scheme, from which the uniqueness of the numerical solution can be inferred. Finally, a dimension-splitting implementation scheme of the separation-of-variables type is designed for the CSLDG method based on the tensor product of polynomials to solve two-dimensional transport equations. Numerical experiments confirm the effectiveness of our work.

It is noteworthy that we observed both superconvergence and fluctuations in convergence orders in our numerical experiments. This phenomenon is not caused by our separated variable-type dimensional splitting scheme, as the classical interpolation-based dimensional splitting exhibits the same issues. In fact, this behavior can be observed in Tables 1-3 and Table 7 of the review literature [4]. We conjecture that this may be related to inherent properties of the CSLDG algorithm itself and the use of CFL numbers exceeding 1. Although previous numerical experiments using CSLDG with interpolation-based splitting for transport equations have encountered this phenomenon, these studies did not investigate its underlying causes. Therefore, a more detailed and rigorous mathematical explanation may become the focus of our subsequent research.

Acknowledgments The authors would like to thank the anonymous referees for their very valuable comments and suggestions.

Declarations

Conflict of interest The authors have no conflict of interest to declare that are relevant to the content of this article.

Funding Not applicable. There was no funding for this paper.

Data Availability Data can be provided from the corresponding author on reasonable request.

Author contribution Not applicable. There is only one author.

References

[1] GUO W, NAIR R D, QIU J-M. A Conservative Semi-Lagrangian Discontinuous Galerkin Scheme on the Cubed Sphere [J]. Monthly Weather Review, 2014, 142(1): 457-75. 1, 1, 1, 1, 2.3, 4.2

[2] CELIA M A, RUSSELL T F, HERRERA I, et al. An Eulerian-Lagrangian localized adjoint method for the advection-diffusion equation [J]. Advances in Water Resources, 1990, 13(4): 187-206. 1, 1

[3] CAI X, GUO W, QIU J. A High Order Conservative Semi-Lagrangian Discontinuous Galerkin Method for Two-Dimensional Transport Simulations [J]. Journal of Scientific Computing, 2017, 73. 1, 2.3

[4] CAI X, GUO W, QIU J-M. Comparison of Semi-Lagrangian Discontinuous Galerkin Schemes for Linear and Nonlinear Transport Simulations [J]. Communications on Applied Mathematics and Computation, 2019, 4: 3 - 33. 1, 1, 4.2, 6

[5] CAI X, QIU J-M. Eulerian–Lagrangian Runge–Kutta Discontinuous Galerkin Method for Transport Simulations on Unstructured Meshes [J]. SIAM Journal on Scientific Computing, 2022, 44(4): A2037-A60. 1

[6] CAI X, LI Q, LIU H, et al. A high-order energy-conserving semi-Lagrangian discontinuous Galerkin method for the Vlasov-Ampère system [J]. Acta Mechanica Sinica, 2025. 1

[7] CAI X, KONG L, KUZMIN D, et al. Asymptotic-preserving conservative semi-Lagrangian discontinuous Galerkin schemes for the Vlasov-Poisson system in the quasi-neutral limit [J]. arXiv preprint arXiv: 2510.15854, 2025. 1

[8] DING M, CAI X, GUO W, et al. A semi-Lagrangian discontinuous Galerkin (DG) - local DG method for solving convection-diffusion equations [J]. Journal of Computational Physics, 2020, 409: 109295. 1

[9] CAI X, BOSCARINO S, QIU J. High order semi-Lagrangian discontinuous Galerkin method coupled with Runge-Kutta exponential integrators for nonlinear Vlasov dynamics [J]. Journal of Computational Physics, 2020, 427: 110036. 1, 2.3

[10] CAI X, GUO W, QIU J. A High Order Semi-Lagrangian Discontinuous Galerkin Method for the Two-Dimensional Incompressible Euler Equations and the Guiding Center Vlasov Model Without Operator Splitting [J]. Journal of Scientific Computing, 2019, 79. 1, 2.3

[11] YOUNES A, ACKERER P. Solving the advection-diffusion equation with the Eulerian-Lagrangian localized adjoint method on unstructured meshes and non uniform time stepping [J]. Journal of Computational Physics, 2005, 208(1): 384-402. 1

[12] RUSSELL T F, CELIA M A. An overview of research on Eulerian-Lagrangian localized adjoint methods (ELLAM) [J]. Advances in Water Resources, 2002, 25(8): 1215-31. 1

[13] QIU J-M, SHU C-W. Positivity preserving semi-Lagrangian discontinuous Galerkin formulation: Theoretical analysis and application to the Vlasov-Poisson system [J]. Journal of Computational Physics, 2011, 230(23): 8386-409. 1, 4.1

[14] RESTELLI M, BONAVENTURA L, SACCO R. A semi-Lagrangian discontinuous Galerkin method for scalar advection by incompressible flows [J]. Journal of Computational Physics, 2006, 216(1): 195-215. 1

[15] YANG Y, CAI X, QIU J-M. Optimal convergence and superconvergence of semi-Lagrangian discontinuous Galerkin methods for linear convection equations in one space dimension [J]. Mathematics of Computation, 2020, 89: 2113-39. 1

[16] FALCONE M, FERRETTI R. Convergence Analysis for a Class of High-Order Semi-Lagrangian Advection Schemes [J]. SIAM Journal on Numerical Analysis, 1998, 35(3): 909-40. 1

[17] WEI H, HOU Y. Dimension Splitting Algorithms for Three Dimensional Steady/Unsteady Stokes Equations [J]. Chinese Journal of Engineering Mathematics, 2015, 32(3): 445-461. DOI: 10.3969/j.issn.1005-3085.2015.03.013. 1

[18] GU C-H, LI D-Q, CHEN S-X, ZHENG S-M, TAN Y-J. Mathematical Physics Equations [M]. 3rd ed. HIGHER EDUCATION PRESS BEIJING. 2012: Chapter 5, pp. 138-142. 2.4

[19] PONTRYAGIN L S. Ordinary Differential Equations [M]. Pergamon, 1962: Chapter 3, pp. 127-149. 3.1

[20] STRANG G. On the Construction and Comparison of Difference Schemes [J]. SIAM Journal on Numerical Analysis, 1968, 5: 506-17. 4.1

[21] FOREST E, RUTH R D. Fourth-order symplectic integration [J]. Physica D: Nonlinear Phenomena, 1990, 43(1): 105-17. 4.1

[22] YOSHIDA H. Construction of higher order symplectic integrators [J]. Physics Letters A, 1990, 150(5): 262-8. 4.1

[23] YOSHIDA H. Recent progress in the theory and application of symplectic integrators [J]. Celestial Mechanics and Dynamical Astronomy, 1993, 56(1): 27-43. 4.1

Appendix A. Differentiation formula for variable-limit integrals(Leibniz Rule)

$\Omega(t)$ denotes a time-dependent bounded domain, and at time t^*, $\Omega(t)$ is fixed as $\Omega_t^\star$, i.e., $\Omega_t^\star = \Omega(t^\star)$. Let $\frac{\mathrm{d}}{\mathrm{d}t}(\cdot)$ represent the material derivative (substantial derivative), and denote $\mathbf{u} = \frac{\mathrm{d}\mathbf{x}}{\mathrm{d}t}$. The differentiation formula for integrals with variable limits (also known as the Leibniz rule) is given by:

- For a scalar function $f(\mathbf{x},t) : \mathbb{R}^d \times [0,+\infty] \longrightarrow \mathbb{R}$,

$$\frac{\mathrm{d}}{\mathrm{d}t}\left[\int_{\Omega(t)} f(\mathbf{x},t)\,\mathrm{d}\mathbf{x}\right] = \int_{\Omega_t^\star} \frac{\partial f}{\partial t} + \nabla\cdot\left(f\cdot\frac{\mathrm{d}\mathbf{x}}{\mathrm{d}t}\right)\mathrm{d}\mathbf{x} = \int_{\Omega_t^\star} \frac{\partial f}{\partial t} + \nabla\cdot(f\cdot\mathbf{u})\,\mathrm{d}\mathbf{x}. \tag{A.1}$$

- For a vector function $\mathbf{F}(\mathbf{x},t) : \mathbb{R}^d \times [0,+\infty] \longrightarrow \mathbb{R}^d$,

$$\frac{\mathrm{d}}{\mathrm{d}t}\left[\int_{\Omega(t)} \mathbf{F}(\mathbf{x},t)\ \mathrm{d}\mathbf{x}\right] = \int_{\Omega_t^\star} \frac{\partial \mathbf{F}}{\partial t} + \nabla\cdot(\mathbf{F}\otimes\frac{\mathrm{d}\mathbf{x}}{\mathrm{d}t})\ \mathrm{d}\mathbf{x} = \int_{\Omega_t^\star} \frac{\partial \mathbf{F}}{\partial t} + \nabla\cdot(\mathbf{F}\otimes\mathbf{u})\ \mathrm{d}\mathbf{x}, \tag{A.2}$$

  where "$\otimes$" denotes the "Kronecker product" between vectors, defined as:

$$\mathbf{a}\otimes\mathbf{b} = \mathbf{a}\mathbf{b}^{\mathrm{T}} = \begin{bmatrix} a_1 \\ a_2 \\ a_3 \end{bmatrix}[b_1,b_2,b_3] = \begin{bmatrix} a_1b_1 & a_1b_2 & a_1b_3 \\ a_2b_1 & a_2b_2 & a_2b_3 \\ a_3b_1 & a_3b_2 & a_3b_3 \end{bmatrix}. \tag{A.3}$$

Remark A.1. *Starting from the equation (A.1), and using the divergence theorem, we obtain*

$$\begin{aligned}\frac{\mathrm{d}}{\mathrm{d}t}\left[\int_{\Omega(t)} f(\mathbf{X},t)\,\mathrm{d}\mathbf{X}\right] &= \int_{\Omega_t^\star}\frac{\partial f}{\partial t} + \int_{\Omega_t^\star}\nabla\cdot(\mathbf{u}\cdot f)\,\mathrm{d}\mathbf{X} \\ &= \int_{\Omega_t^\star}\frac{\partial f}{\partial t} + \int_{\partial\Omega_t^\star}\mathbf{n}\cdot(\mathbf{u}\cdot f)\,\mathrm{d}\sigma(\mathbf{X}) \\ &= \int_{\Omega_t^\star}\frac{\partial f}{\partial t} + \int_{\partial\Omega_t^\star} f(\mathbf{n}\cdot\mathbf{u})\,\mathrm{d}\sigma(\mathbf{X}),\end{aligned}$$

where $\mathbf{n}$ *is the unit outward normal vector to* $\partial\Omega_t^\star$*, and the last equality is the* ***Reynolds transport theorem****.*

(Z. Xie) School of Mathematical Sciences, East China Normal University, Shanghai 200241, China

Email address: xzr_nature@163.com; 52265500018@stu.ecnu.edu.cn